High and Low-Multiplicity pp-Collisions and Long-Range Angular Correlations

Report by G.Feofilov at LUHEP seminar May 14, 2024,
Petergof , 12:00—13:00

- Яркий сигнал процесса слияния кварк-глюонных струн?

Layout

- Emergence of Long-Range Angular Correlations in Low-Multiplicity Proton-Proton Collisions(PHYSICAL REVIEW LETTERS 132, 172302 (2024))—кратко
- Percolation string model and old predictions for critical beaviour -- where to search for the critical point
- High and Low-Multiplicity pp-Collisions and Long-Range Angular Correlations
- Plans

Emergence of Long-Range Angular Correlations in Low-Multiplicity Proton-Proton Collisions

S. Acharya et al.*
(ALICE Collaboration)

This Letter presents the measurement of near-side associated per-trigger yields, denoted ridge yields, from the analysis of angular correlations of charged hadrons in proton-proton collisions at $\sqrt{s} = 13$ TeV. Long-range ridge yields are extracted for pairs of charged particles with a pseudorapidity difference of $1.4 < |\Delta\eta| < 1.8$ and a transverse momentum of $1 < p_{\mathrm{T}} < 2$ GeV/c, as a function of the charged-particle multiplicity measured at midrapidity. This Letter extends the measurements of the ridge yield to the low multiplicity region, where in hadronic collisions it is typically conjectured that a strongly interacting medium is unlikely to be formed. The precision of the new low multiplicity results allows for the first direct quantitative comparison with the results obtained in e^+e^- collisions at $\sqrt{s} = 91$ GeV and $\sqrt{s} = 183$–209 GeV, where initial-state effects such as preequilibrium dynamics and collision geometry are not expected to play a role. In the multiplicity range $8 \lesssim \langle N_{\mathrm{ch}} \rangle \lesssim 24$ where the e^+e^- results have good precision, the measured ridge yields in pp collisions are substantially larger than the limits set in e^+e^- annihilations. Consequently, the findings presented in this Letter suggest that the processes involved in e^+e^- annihilations do not contribute significantly to the emergence of long-range correlations in pp collisions.

PHYSICAL REVIEW LETTERS 132, 172302 (2024)
DOI: 10.1103/PhysRevLett.132.172302

The observables presented in this analysis are extracted using two-particle angular correlations for pairs of charged particles. The two-particle per-trigger yield is measured as a function of relative azimuthal angle $\Delta\varphi$ and pseudorapidity $\Delta\eta$ of two particles—traditionally called trigger and associated—and is defined as

$$\frac{1}{N_{\text{trig}}}\frac{\mathrm{d}^2 N_{\text{pair}}}{\mathrm{d}\Delta\eta\mathrm{d}\Delta\varphi} = B(0,0)\,\frac{S(\Delta\eta,\Delta\varphi)}{B(\Delta\eta,\Delta\varphi)}. \qquad (1)$$

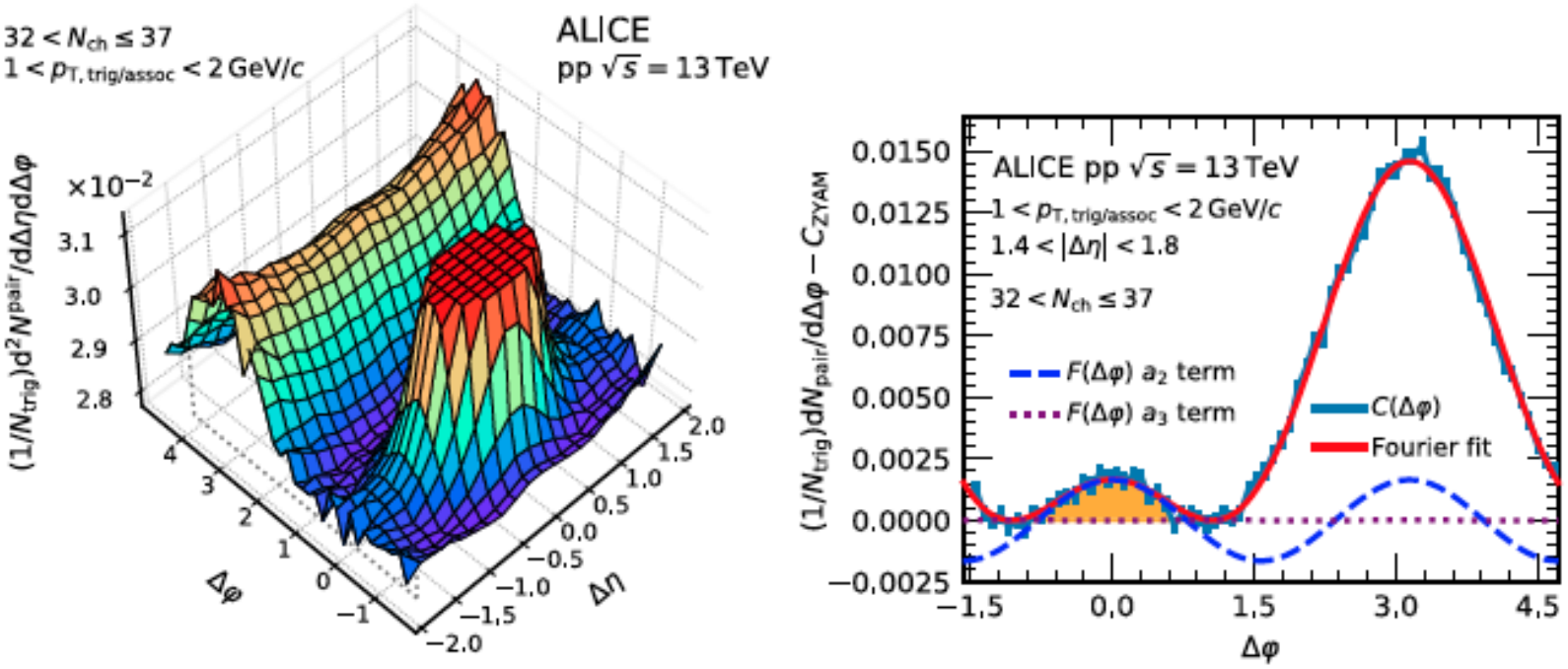

FIG. 1. Two-particle per-trigger yield measured for charged track pairs with $1 < p_{\mathrm{T,trig}} < 2$ GeV/c and $1 < p_{\mathrm{T,assoc}} < 2$ GeV/c within the multiplicity range $32 < N_{\mathrm{ch}} \leq 37$. The jet fragmentation peak has been truncated to ensure a better visibility of the long-range structure. The right panel shows the zero-suppressed projection to $\Delta\varphi$ overlaid with $F(\Delta\varphi)$ (red line) and the area in which the ridge yield is extracted (shaded area). The blue and purple lines represent the second and third harmonic terms of $F(\Delta\varphi)$.

The per-trigger yield distribution as a function of $\Delta\varphi$ is obtained by integrating the two-dimensional two-particle per-trigger yield in the long-range intervals $1.4 < |\Delta\eta| < 1.8$, in order to exclude the region dominated by the jet fragmentation peak

$$Y(\Delta\varphi) = \frac{1}{N_{\text{trig}}}\frac{\mathrm{d}N_{\text{pair}}}{\mathrm{d}\Delta\varphi} = \int_{1.4<|\Delta\eta|<1.8}\left(\frac{1}{N_{\text{trig}}}\frac{\mathrm{d}^2N_{\text{pair}}}{\mathrm{d}\Delta\eta\mathrm{d}\Delta\varphi}\right)\frac{1}{\delta_{\Delta\eta}}\mathrm{d}\Delta\eta, \quad (2)$$

where $\delta_{\Delta\eta} = 0.8$ is the normalization constant for the chosen $\Delta\eta$ range. The ridge yield Y^{ridge} is extracted by integrating the near-side area of the associated per-trigger yield using

$$Y^{\text{ridge}} = \int_{|\Delta\varphi|<|\Delta\varphi_{\text{min}}|} Y(\Delta\varphi)\mathrm{d}\Delta\varphi - 2|\Delta\varphi_{\text{min}}|C_{\text{ZYAM}}. \quad (3)$$

Ridge yield as a function of $\langle N_{ch} \rangle$

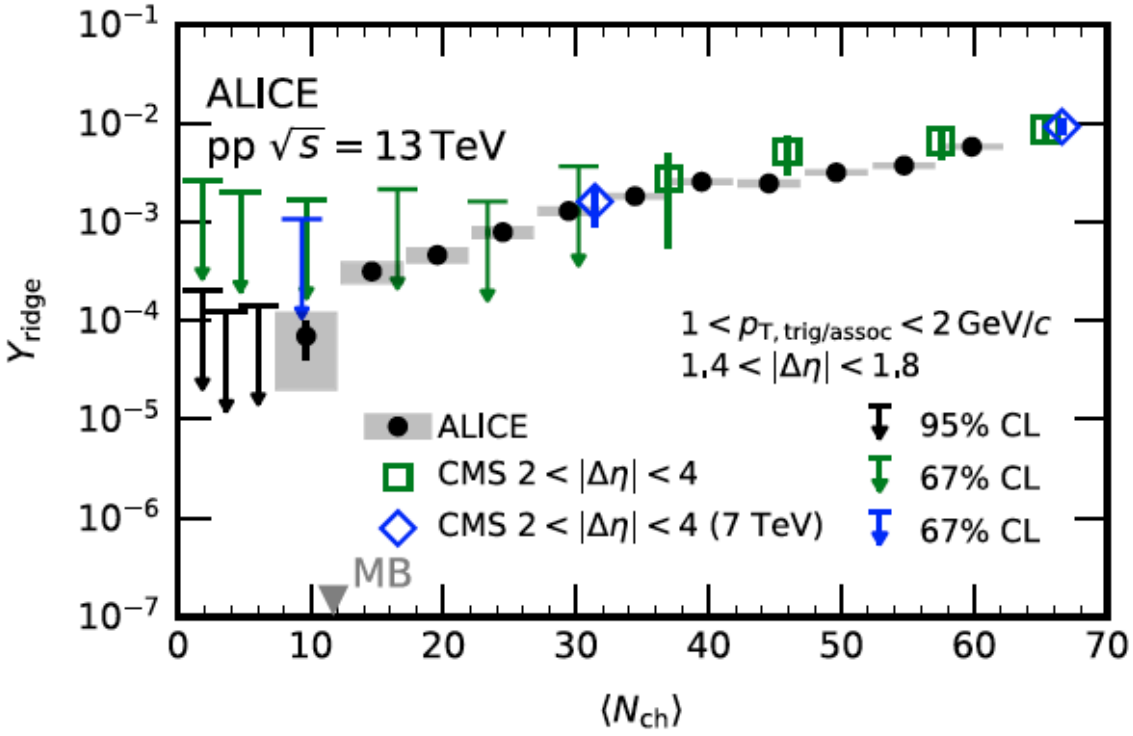

FIG. 2. Ridge yield as a function of multiplicity. The black points correspond to the measurement presented in this Letter, while data from CMS [8,38] are drawn as green and blue markers. Vertical bars denote statistical uncertainties while systematic uncertainty is shown as a shaded area. For both results, at low multiplicity where the lower uncertainty reaches zero, an upper limit is reported, which is drawn as a bar and down arrow. Such points are given at 95% CL for the results from this Letter and at 67% for the results from CMS. The "MB" arrow at $\langle N_{ch} \rangle = 11.3$ indicates the multiplicity averaged over the entire studied multiplicity range.

Comparison to e+e- collisions

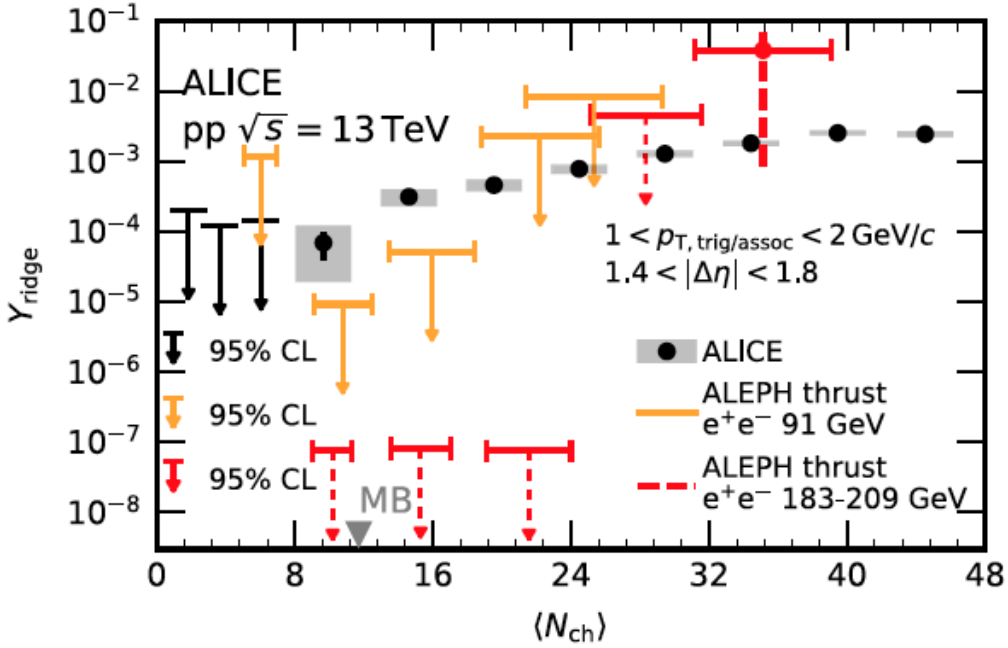

FIG. 3. Ridge yield as a function of multiplicity, compared to the upper limits on the ridge yield in e^+e^- collisions. Vertical bars denote statistical uncertainties while systematic uncertainty is shown as the shaded areas. The orange limits represent the measurement in the thrust-axis reference frame with ALEPH [34]. The horizontal bars in the ALEPH points represent the uncertainty related to the multiplicity conversion from the ALEPH to the ALICE acceptance (see text). All limits are given at 95% CL.

In the multiplicity range 8 to 18 (24) the yields in pp collisions are substantially above the ALEPH limit at $\sqrt{s} = 91$ ($\sqrt{s} = 183$–209 GeV) while outside this range the limits from e^+e^- collisions are above the pp measurement.

Similarly to the previous figure, in order to translate the ALEPH multiplicity into the ALICE acceptance range, a scaling factor is estimated with PYTHIA8.3 events by counting the resulting particles in the acceptance ranges of both experiments ($|\eta| < 1.738$, $p_{\mathrm{T}} > 0.2$ GeV/c in case of ALEPH).

e+e-

In Fig. 3, the result is compared to a recent measurement performed in e^+e^- collisions at $\sqrt{s} = 91$ [34] and at $\sqrt{s} =$ 183–209 GeV [35] in the thrust-axis reference frame using ALEPH archived data.

Because of the absence of beam remnants, the thrust axis provides an estimate of the longitudinal color field between the initially created outgoing $q\bar{q}$ pair and is therefore the sensible choice in e^+e^- collisions to search for collective effects.

Compare to MC

[redacted] This suggests that the mechanisms for ridge yield production in very small hadronic collisions have not been understood and more theoretical work is needed.

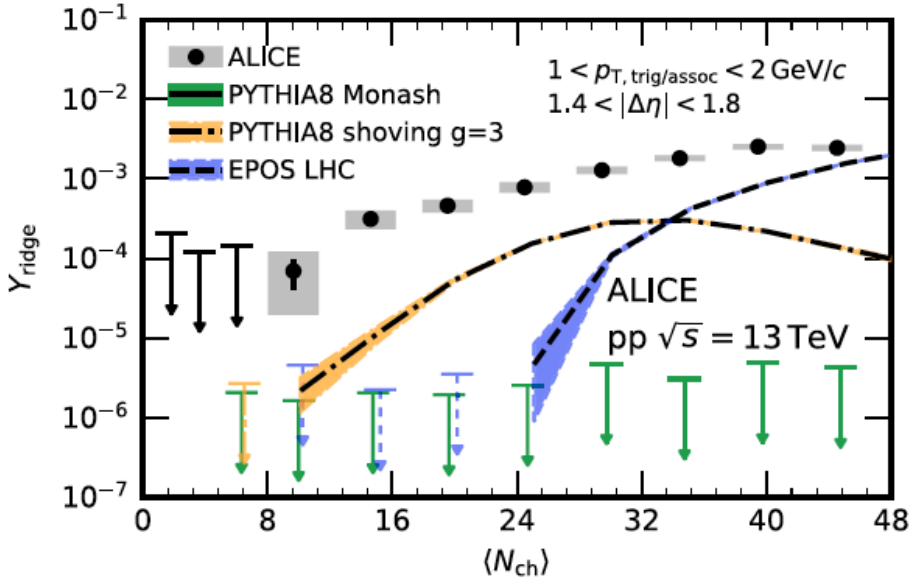

[redacted]. The results presented in this Letter suggest that the ridge yield measured from a hadronic system of roughly equivalent multiplicity is nonzero and substantially larger than the limit observed in e^+e^- annihilations. Based on this, one can conclude that additional processes besides those in the e^+e^- annihilations must play a role for the emergence of long-range correlations in pp collisions.

- Очень странный вывод !
- Пытаются сопоставлять эффекты дальних корреляций для e+e- и pp, основываясь на такой наблюдаемой как множественность ???
- Некорректный подход??? Разные механизмы адронизации в процессах e+e- и pp

- Emergence of Long-Range Angular Correlations in Low-Multiplicity Proton-Proton Collisions(PHYSICAL REVIEW LETTERS 132, 172302 (2024))—кратко
- Percolation string model and old predictions for critical beaviour -- where to search for the critical point
- High and Low-Multiplicity pp-Collisions and Long-Range Angular Correlations
- Plans

O.Kochebina and G.Feofilov, Onset of ”ridge phenomenon” in AA and pp collisions and percolation string modelarXiv:1012.0173v1

New phenomena in AA collisions observed by STAR [1]

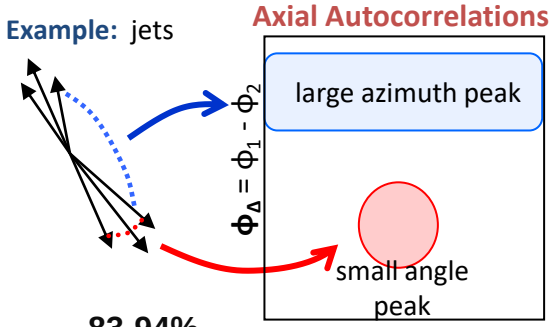

Variation of low-p_T "ridge" with centrality (Npart).

(pt> 0.15 GeV/c)

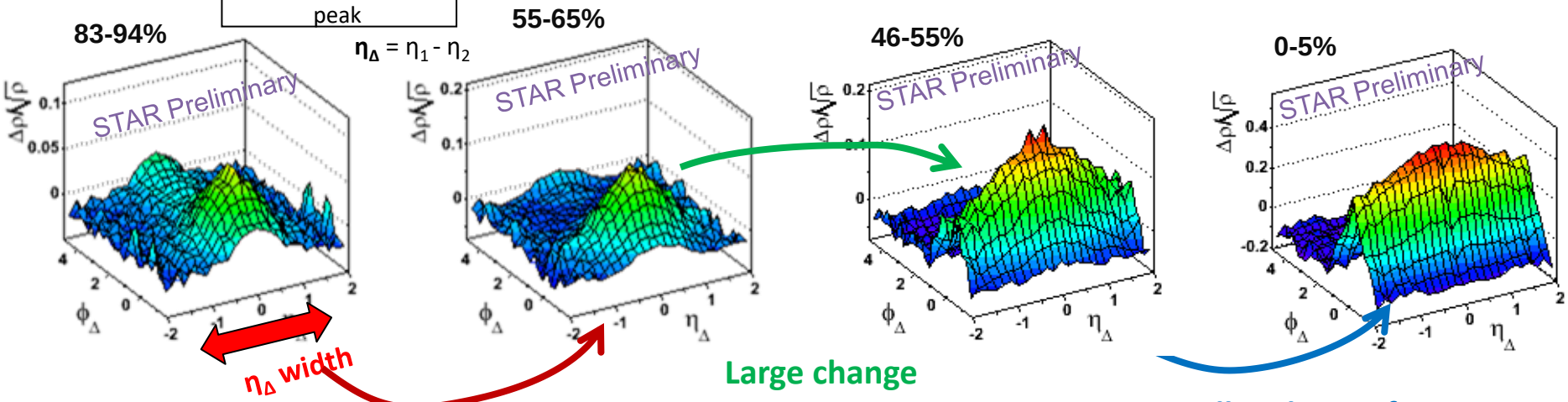

Shape changes little from peripheral to the transition

Large change within ~10% centrality

Smaller change from transition to most central

Low-p_T manifestation of the "ridge"

The data showed a sharp transition at some definite energy-dependent centrality: **growing of peak amplitude** and **stretching of width**.

[1]Anomalous centrality variation of minijet angular correlations in Au-Au collisions at 62 and 200 GeV from STAR. M. Daugherity(QM2008), J.Phys.G35:104090,2008

Variation of low-p_T "ridge" with centrality (Npart).

A sudden increase of the **peak amplitude** and **η width** of ***the near-side low p_t ridge*** were found at an *energy-dependent* centrality point at definite number of participating nucleons **Npart**.

N_{part}

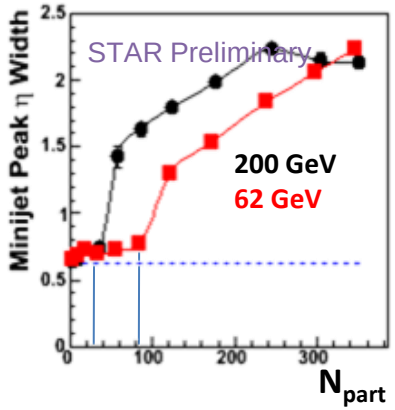

Transverse Particle Density

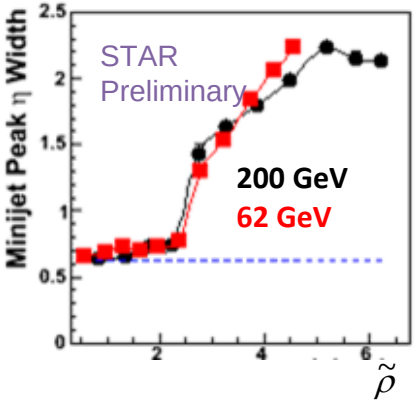

$$\tilde{\rho} = \frac{3}{2}\frac{dN_{ch}}{d\eta} / S$$

62 GeV

"Critical value" N_{part}≈90

200 GeV

"Critical value" N_{part}≈40

$$\tilde{\rho}_{crit} = 2{,}6 \pm 0{,}2\ fm^{-2}$$

Same-side gaussian peak width. Points show eleven centrality bins for each energy (84-93%, 74-84%, 65-74%, 55-65%, 46-55%, 37-46%, 28-37%, 19-28%, 9-19%, 5-9%, and 0-5%) transformed to tranvserse density.

Anomalous centrality variation of minijet angular correlations in Au-Au collisions at 62 and 200 GeV from STAR. M. Daugherity. QM2008, J.Phys.G35:104090,2008

Variation of low-p_T "ridge" with centrality (Npart).

A sudden increase of the **peak amplitude** and **η width** of ***the near-side low p_t ridge*** were found at an *energy-dependent* centrality point at definite number of participating nucleons **Npart**.

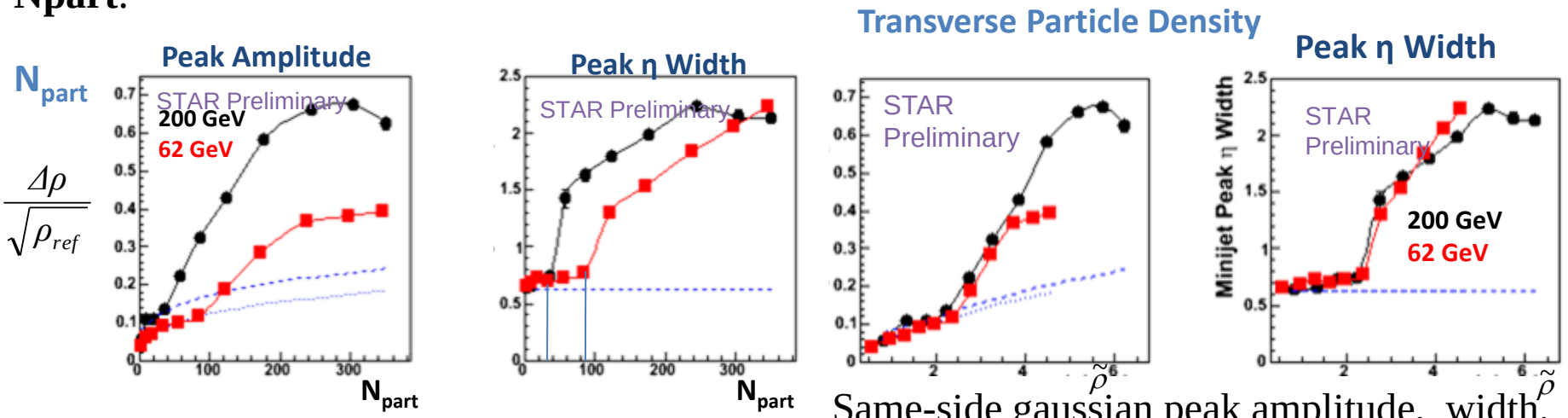

62 GeV
"Critical value" Npart≈90

200 GeV
"Critical value" Npart≈40

Same-side gaussian peak amplitude, width. Points show eleven centrality bins for each energy (84-93%, 74-84%, 65-74%, 55-65%, 46-55%, 37-46%, 28-37%, 19-28%, 9-19%, 5-9%, and 0-5%) transformed to tranvserse density.

$$\tilde{\rho} = \frac{3}{2}\frac{dN_{ch}}{d\eta} / S$$

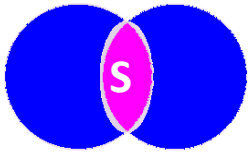

$$\tilde{\rho}_{crit} = 2{,}6 \pm 0{,}2\ fm^{-2}$$

Anomalous centrality variation of minijet angular correlations in Au-Au collisions at 62 and 200 GeV from STAR. M. Daugherity. QM2008.

New! Our calculation

Percolation model parameters at **the "critical" point**

Percolation sting theory[3]

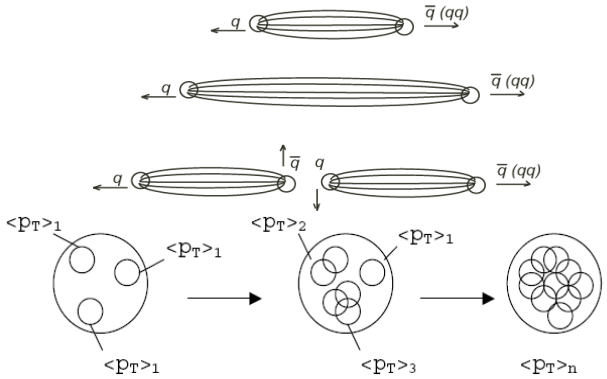

Transverse particle density

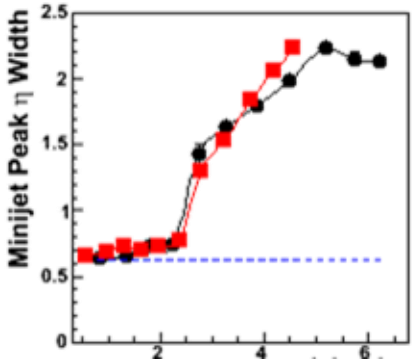

$\tilde{\rho}$

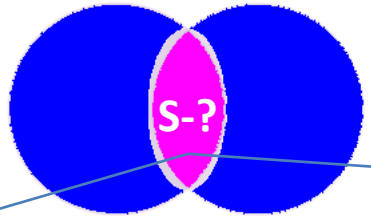

$$n = N_{string}\pi r_0^2 / S$$

$$\tilde{\rho} = \frac{3}{2}\frac{dN_{ch}}{d\eta} / S$$

$$n_{crit} = 1{,}12 - 1{,}175 [4]$$

$$\frac{\tilde{\rho}_{crit}}{n_{crit}}$$

$$\tilde{\rho}_{crit} = 2{,}6 \pm 0{,}2\ fm^{-2} [1]$$

Parameters of the model

[3] C. Pajares // arXiv:hep-ph/0501125v1 14 Jan 2005

[4] N. Armesto, M.A, Braun, E.G. Ferreiro, C. Pajares// Phys. Rev. Lett. 77, 3736 (1996)

[5]V.V. Vechernin, R.S. Kolevatov, 2007, Yad. Fiz., 2007, Vol. 70, No. 10, pp. 1858–1867.

String model. Estimate of string percolation parameter.

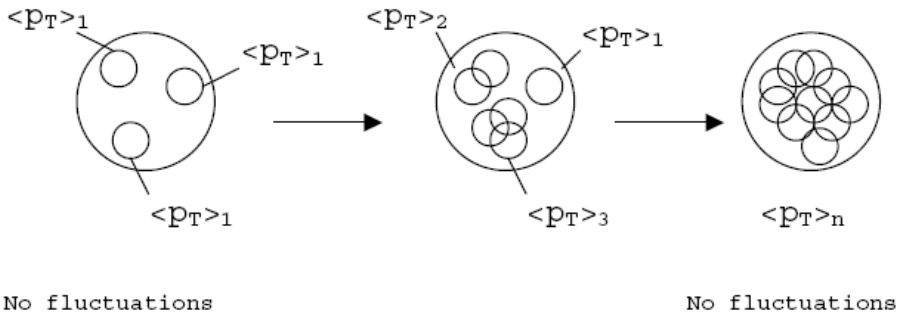

With growing energy and/or atomic number of colliding particles, the number of strings grows and they start to overlap, forming clusters, **new type of particle emitting source**.

At a critical density a macroscopic cluster appears that marks the percolation phase transition.[3]

Percolation parameter:

$$\eta(b) = \frac{N_{str}(b)\pi r_0^2}{S(b)}$$

Nstr - ?
S - ?

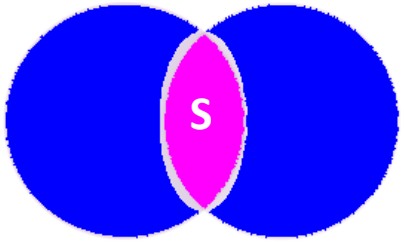

η_c = 1,12-1,175 ([4])

$$N_{str} = N_{Sea} + N_{Valent}$$

$$\eta(N_{part}) = N_{str}(N_{part})\pi r_0^2 / S(N_{part})$$

$$N_{str} = xN_{str}^{(pp)}N_{coll} + (1-x)N_{part}[5]$$

N_{Str} - number of strings, πr_0^2 string transverse area, S overlap area of two nucleons.

r_0**=0,2-0,3 fm** – change of string radius value results in different percolation parameter

[3] C. Pajares // arXiv:hep-ph/0501125v1 14 Jan 2005
[4] N. Armesto, M.A, Braun, E.G. Ferreiro, C. Pajares// Phys. Rev. Lett. 77, 3736 (1996)
[5]V.V. Vechernin, R.S. Kolevatov, 2007, published in Yadernaya Fizika, 2007, Vol. 70, No. 10, pp. 1858–1867.

Transverse particle density vs. percolation parameter

Modified Glouber Model (taken in account momentum loss) [6]

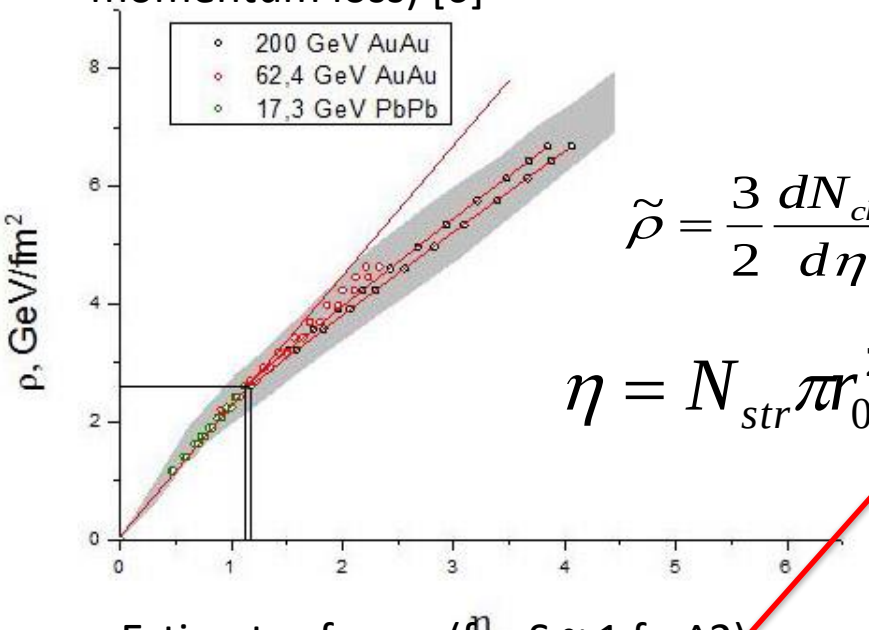

$$\tilde{\rho} = \frac{3}{2}\frac{dN_{ch}}{d\eta} / S$$

$$\eta = N_{str}\pi r_0^2 / S$$

Classical Glouber Model

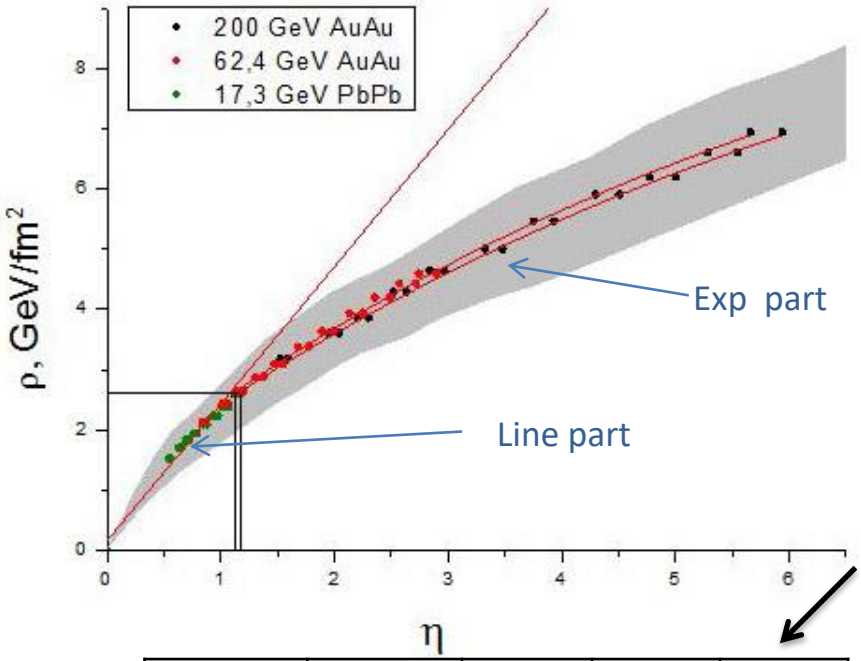

Estimates for pp (for S ~ 1 fm^2):

√s, GeV	dNch/dy[7]	ρ, GeV/fm²	η	Nstr
7000	**6,02**	**9,0 ±0,5**	**5,8 ±0,5**	**24±2**
2360	**4,68**	**7,0±0,4**	**4,3±0,4**	**18±2**
900	**3,78**	**5,6±0,4**	**3,3±0,3**	**13±1**
200	2,30	3,4±0,3	1,7±0,2	7,1±0,7
130	2,03	3,0±0,2	1,5±0,1	6,0±0,6
62,4	1,64	2,5±0,6	1,1±0,1	4,4±0,5
19,4	1,17	1,8±0,5	0,8±0,1	3,1±0,3
17,3	1,14	1,7±0,3	0,7±0,1	3,0±0,3

√s, GeV	dNch/dy[7]	ρ, GeV/fm²	η	Nstr
7000	**6,02**	**9,0±0,5**	**10,4±0,9**	**42±4**
2360	**4,68**	**7,0±0,4**	**6,1±0,5**	**25±3**
900	**3,78**	**5,6±0,4**	**4,2±0,4**	**17±2**
200	2,30	3,4±0,2	1,9±0,2	7,6±0,8
130	2,03	3,0±0,2	1,5±0,1	6,1±0,6
62,4	1,64	2,5±0,1	1,05±0,09	4,3±0,4
19,4	1,17	1,75±0,09	0,73±0,07	3,0±0,3
17,3	1,14	1,70±0,08	0,70±0,06	2,9±0,3

- For **pp** collision the threshold would appear at energy 70-85 GeV.

[6] G.Feofilov,A.Ivanov //Journal of Physics: Conference Series 5 (2005) 230–237

[7] ALICE Collaboration: arXiv:1004.3034[hep-ex], arXiv: 1004.3514[hep-ex]

Ridge in pp

String density in pp collisions

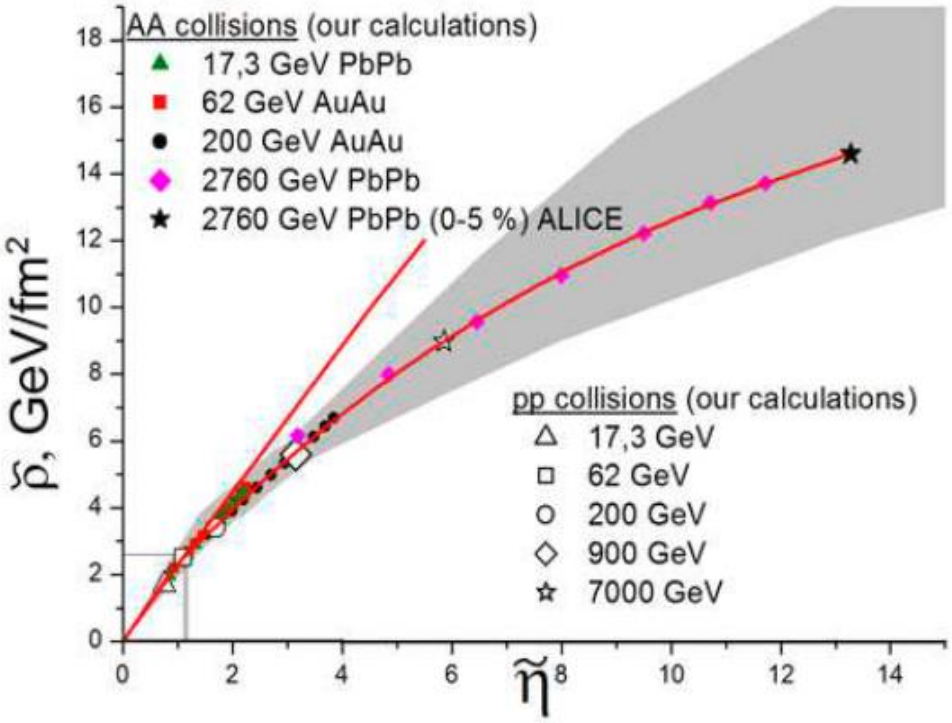

Figure 4: Transverse particle density $\tilde{\rho}$ vs. string density $\tilde{\eta}$ in AA collisions for energy $\sqrt{s} = 17.3$ GeV, $\sqrt{s} = 62$, $\sqrt{s} = 200$ GeV and $\sqrt{s} = 2.76$ TeV. Points are our calculations. Lines are fits to the points. Points for pp collisions are obtained from the experimental data in the range of energies from $\sqrt{s} = 17.3$ GeV to $\sqrt{s} = 7$ TeV (see text).

O.Kochebina and G.Feofilov, Onset of ”ridge phenomenon” in AA and pp collisions and percolation string model, arXiv:1012.0173v1

Azimuthal flow in hadron collisions from quark-gluon string repulsion

Igor Altsybeev, Grigory Feofilov
St.Petersburg State University

Quarks-2016
19th International Seminar on High Energy Physics

May 31, 2016

Unexplained long-range correlations – “Ridge” by CMS in p-Pb at LHC – similar to pp and Pb-Pb !

LHC

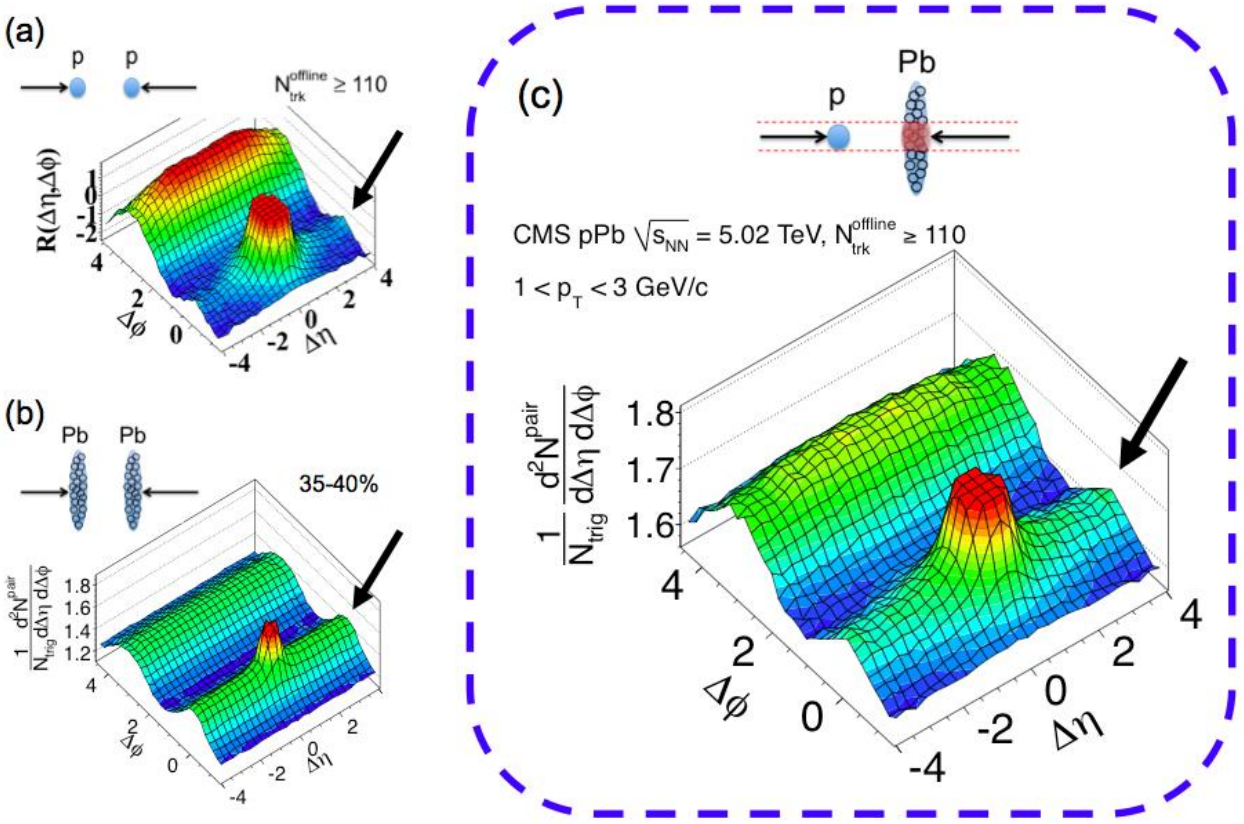

Phys. Lett. B 718 (2013) 795

arXiv:1210.5482 [nucl-ex]

Experiment: Harmonic decomposition of long-range two-particle angular correlations

- shape of the overlap region → large elliptic flow v_2, non-zero v_4
- fluctuations of the initial energy density profile → affect v_2, give v_3, …

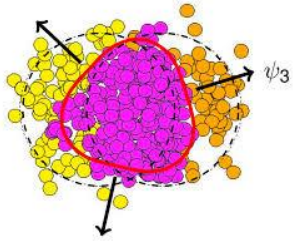

Most central (0-2%) Pb-Pb collisions at 2.76 TeV:

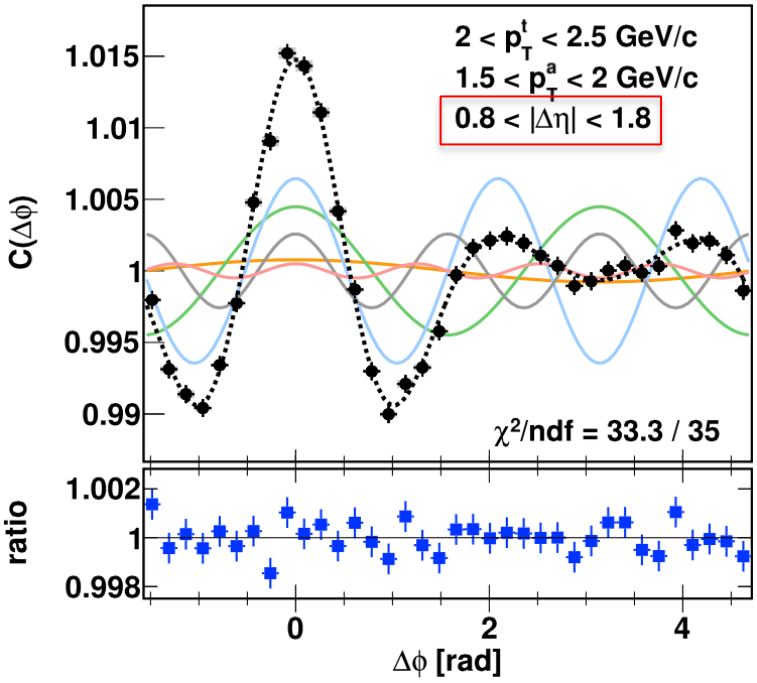

Phys Lett B 708 (2012) 249–264

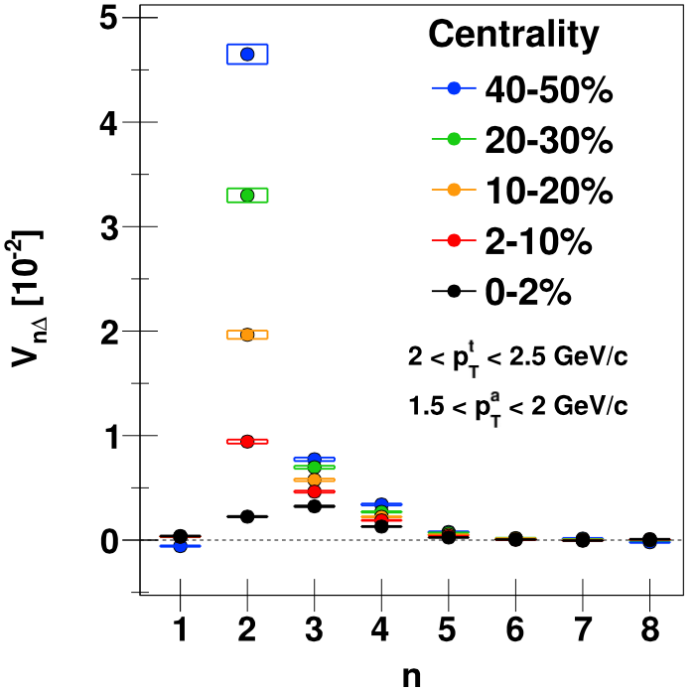

"Double hump" structure – due to larger v_3 relative to v_2 in most central collisions.

Our approach: MC model of repulsive strings*

Assumptions:

- Pair of partons from colliding nucleons can form a string (a color flux tube)
- Strings are repulsing each other within some distance (efficient radius – R_{eff})
- Thus each string gets a summarized momentum kick
- In its rest frame, string decays into particles isotropically in azimuth, but in the lab frame the particles are boosted due to string momentum kick

* see report by I.Altsybeev "Mean transverse momenta correlations in hadron-hadron collisions in MC toy model with repulsing strings" at **Quark Confinement and the Hadron Spectrum XI** 7-12 September 2014 St. Petersburg, arXiv:1502.03608, AIP Conf.Proc. 1701 (2016)

Visualization of a toy event

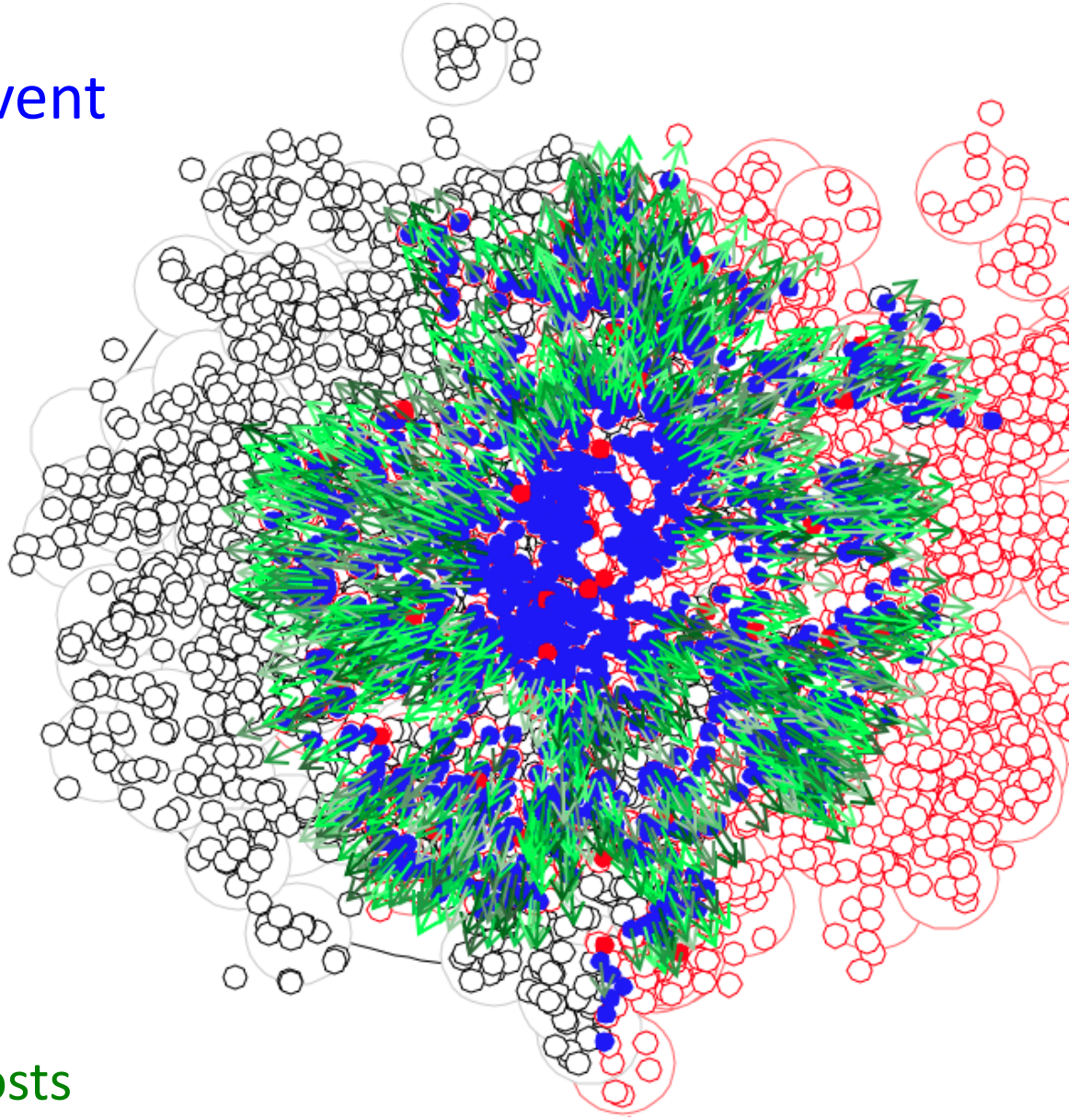

Pb-Pb collision at b=4 fm

blue circles – strings

green arrows – string boosts

Two-particle correlations in MC toy model

MC model results for A-A events at high energies:

(string effective interaction radius is **2 fm**)

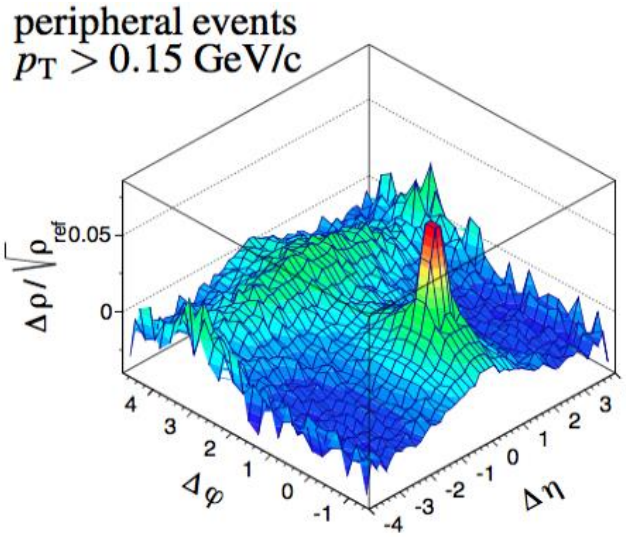

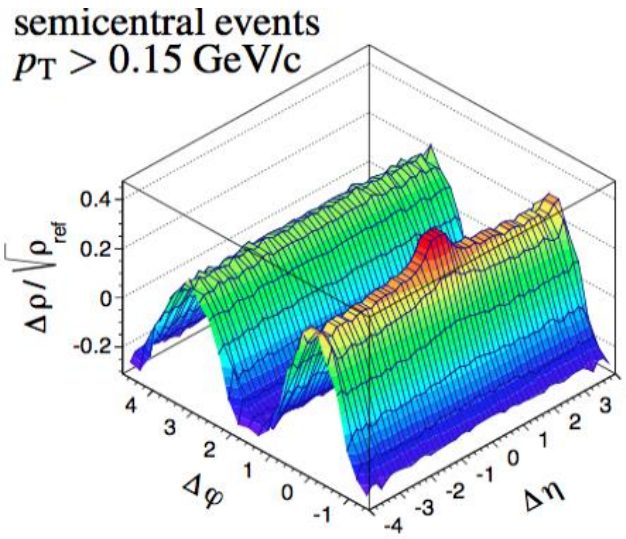

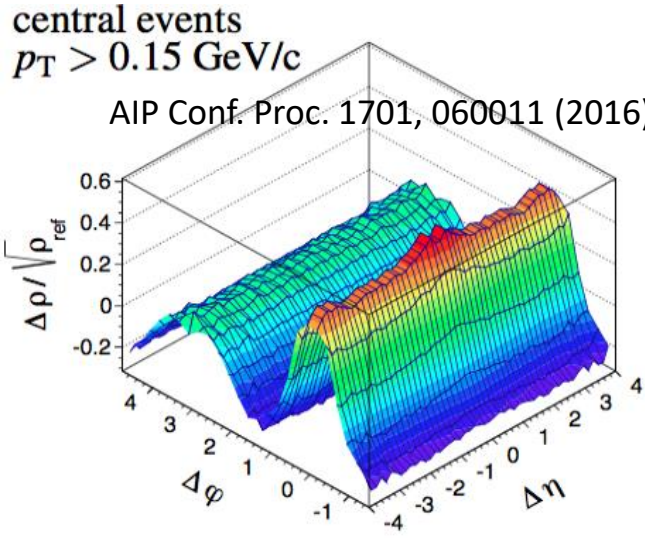

AIP Conf. Proc. 1701, 060011 (2016)

Compare with STAR data (Au-Au):

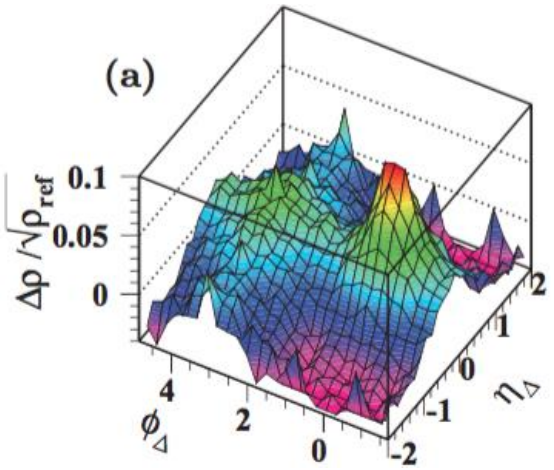

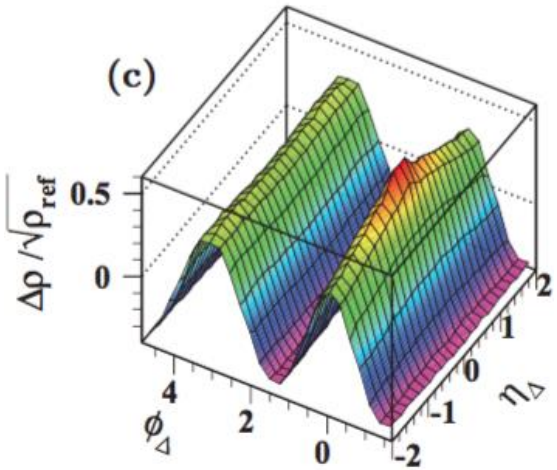

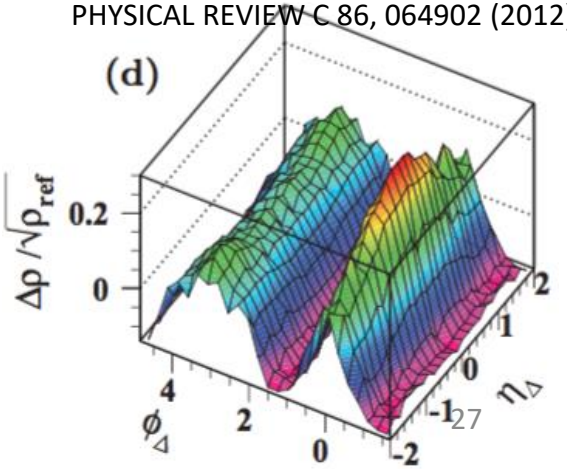

PHYSICAL REVIEW C 86, 064902 (2012)

Our results

G.Feofilov, I.Altsybeev,O.Kochebina, **PoS** (Baldin ISHEPP XXII) 067 (2015)

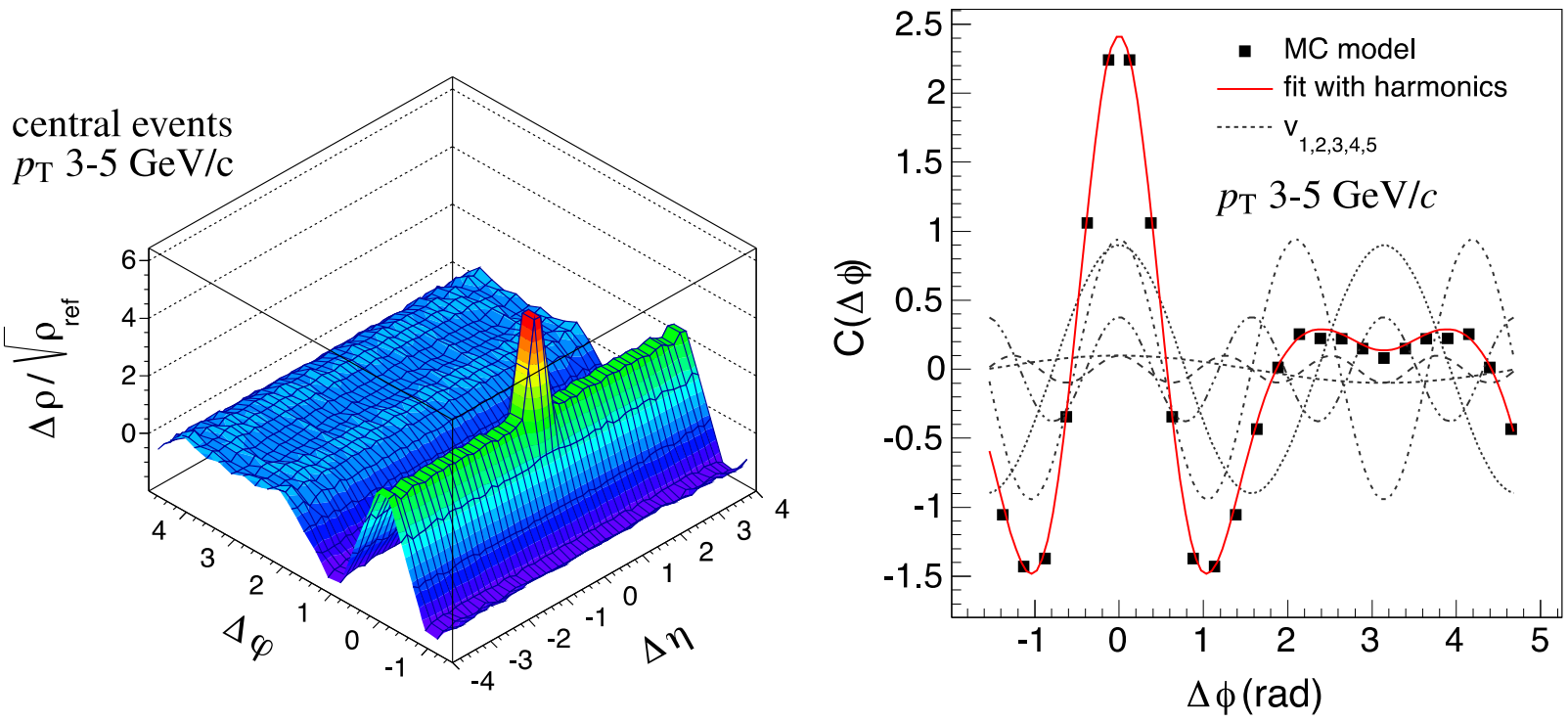

Figure 5: Left: Toy model [19] two-particle correlation function obtained in the most central events for charged particles with $p_T \in [3,5]$ GeV/c. String-string interaction radius R_{int} is 2 fm. Right: The harmonic decomposition of the azimuthal profile of the correlation function shown in the left pad. The solid red line

Radial boost of the strings: influence on p_T spectra

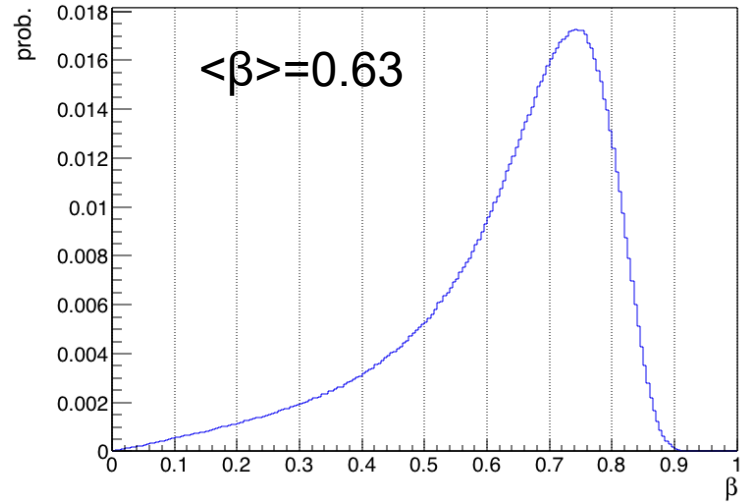

String repulsion leads to some distribution of transverse boosts of the strings.

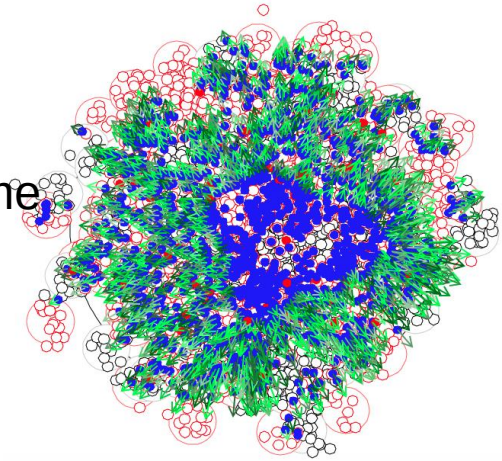

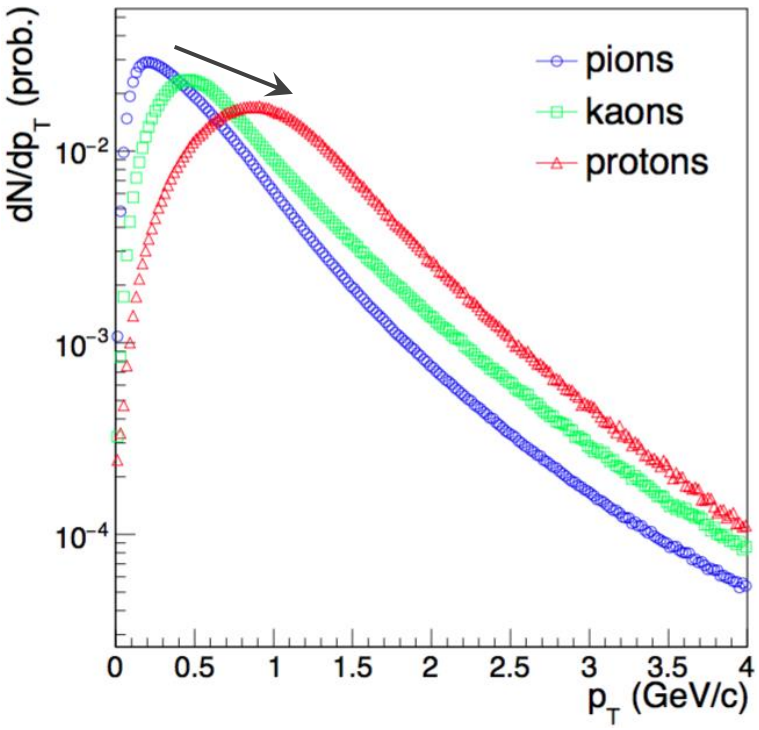

- Particles from strings are boosted in transverse direction.
- More massive particles gain more p_T shift. - harderning of spectrum for protons may be observed

compare to ALICE data →

Bulk particle production in Pb-Pb

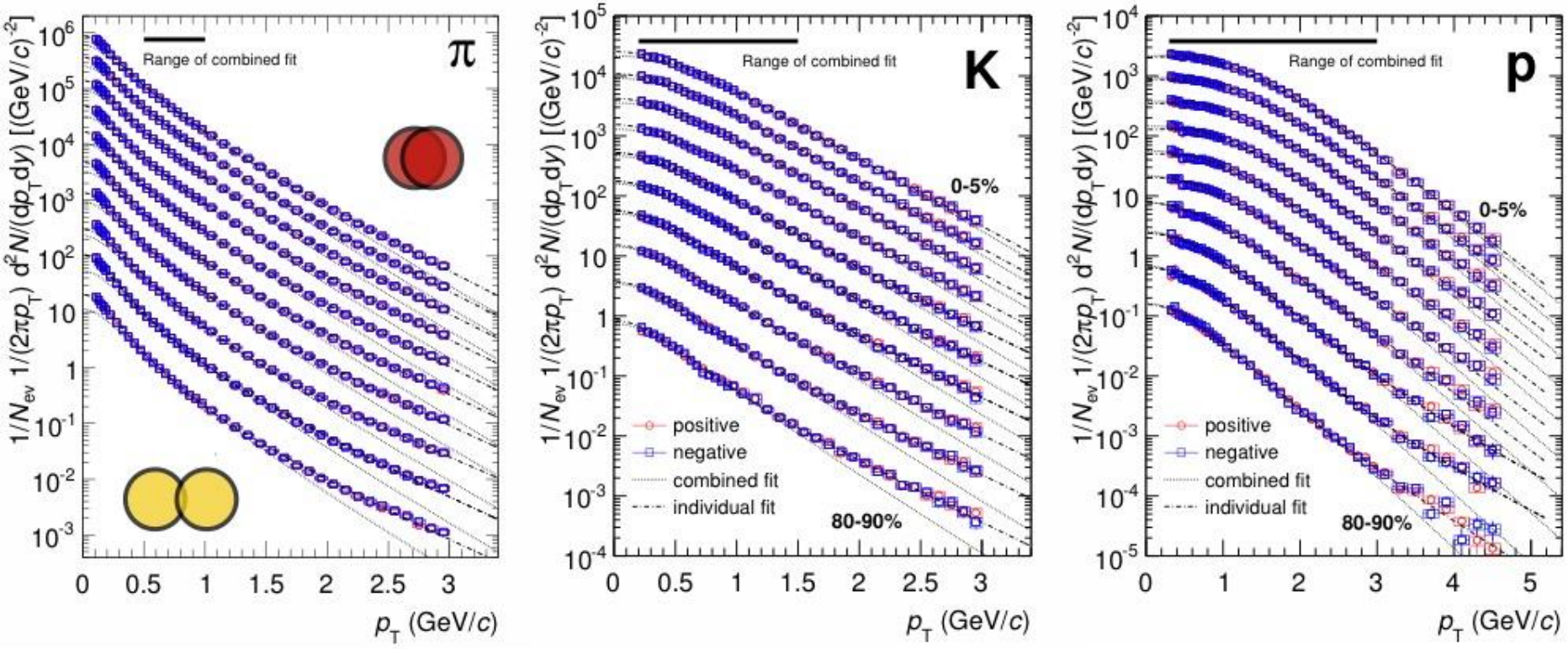

clear evolution of particle spectra → hardening with centrality
more pronounced for protons than for pions
mass ordering as expected from collective hydro expansion

ALICE, PRC 88 (2013) 044910

Differential flow of charged particles

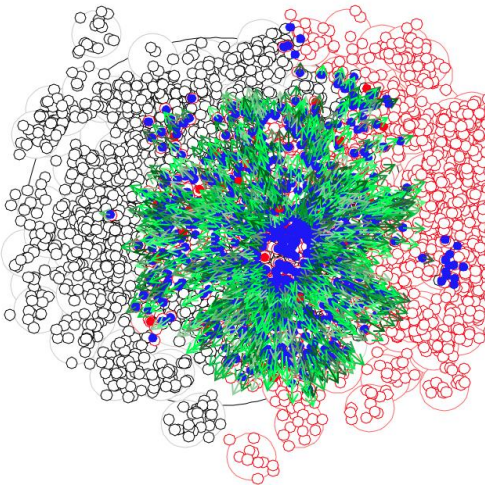

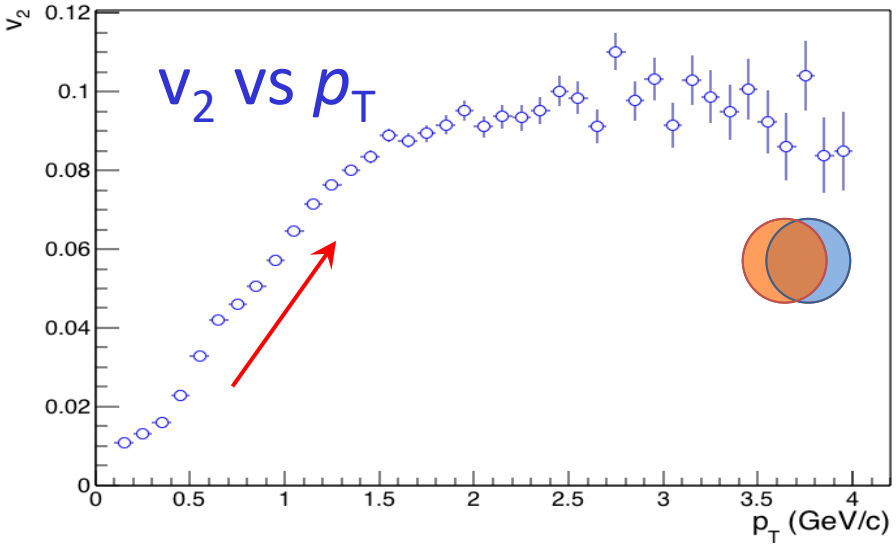

- Qualitative behavior of $v_2(p_T)$ is reproduced in MC model
- "Mass ordering" – to be checked

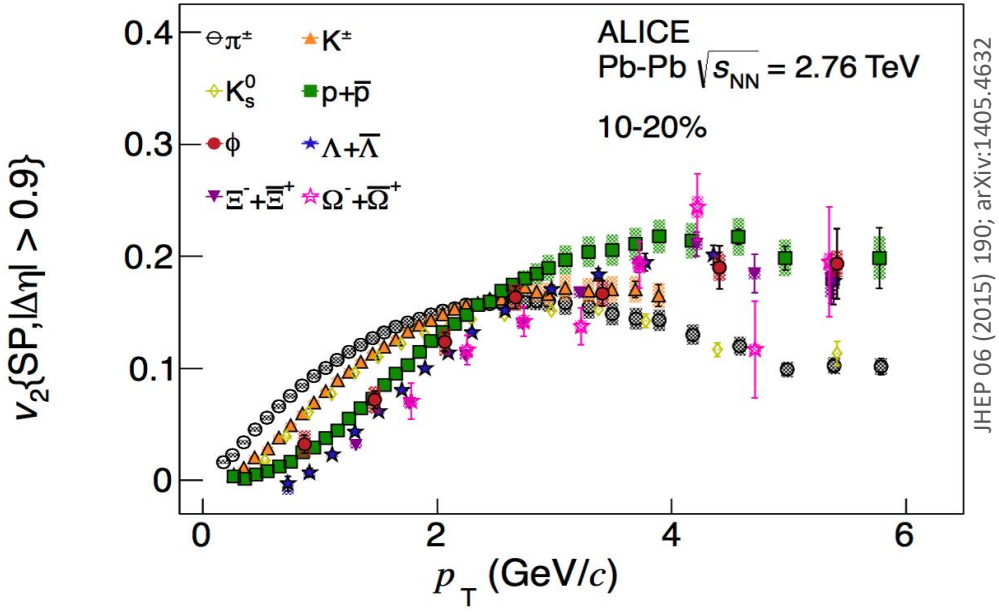

“Mass ordering” in MC model with repulsive strings

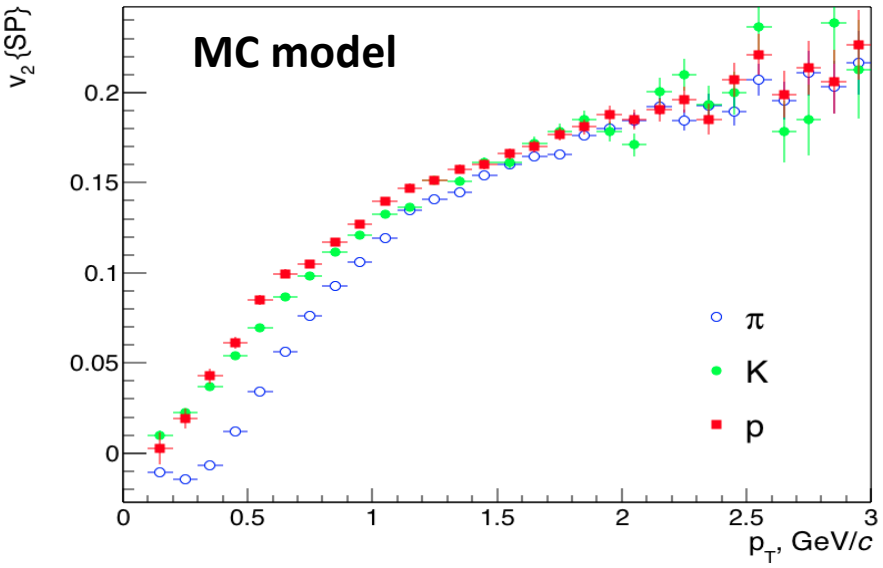

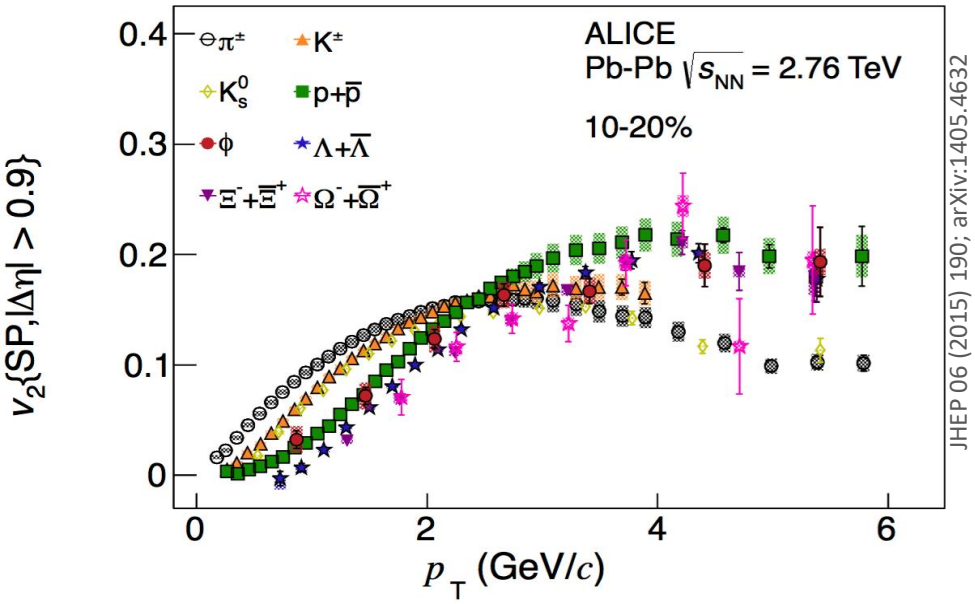

- Qualitative behavior of $v_2(p_T)$ is reproduced in the MC model
- However, “mass ordering” is NOT properly reproduced
  (compare with ALICE results)

→ modifications of the model are needed

Possible modifications:

- "dynamical motion" of strings
- “quenching” of hadrons in medium

Conclusions

- High density string medium could be formed in hadronic collisions.
- It is shown in Monte Carlo toy-model that collective effects appear due to (rather weak) repulsive type of string interaction between color flux tubes (strings): the particle-emitting sources (strings) are boosted by the combined repulsion by neighbours.
- Thus the initial space anisotropy is converted into the harmonics of azimuthal momenta distributions of charged particles.
- Similar results are expected at sufficiently high string density collisions (as is expected for **p-Pb** and **pp** collisions **PoS** (Baldin ISHEPP XXII) 067 (2015)).

- …More detailed quantitative analysis including mass ordering of flows, in the case of proton-proton and proton-nucleus collisions, will follow…

Layout

- Emergence of Long-Range Angular Correlations in Low-Multiplicity Proton-Proton Collisions(PHYSICAL REVIEW LETTERS 132, 172302 (2024))—кратко
- Percolation string model and old predictions for critical beaviour -- where to search for the critical point
- High and Low-Multiplicity pp-Collisions and Long-Range Angular Correlations
- Plans

Вопросы:

1) Количество струн в pp-столкновениях большой множественности – струны какого типа?

Доминирование морских струн [1].

2) Плотность морских струн в самых центральных pp-столкновениях и дальние корреляции?
3) $\langle p_T \rangle$-N_{ch} - корреляции

2) $\langle p_T \rangle$-N_{ch} -дальние корреляции

[1] O.Kochebina and G.Feofilov, Onset of ”ridge phenomenon” in AA and pp collisions and percolation string model, arXiv:1012.0173v1

Модель взаимодействующих струн, конечных по быстроте, учитывающая поперечную и продольную динамику (кандидатская Дарьи Прохоровой)

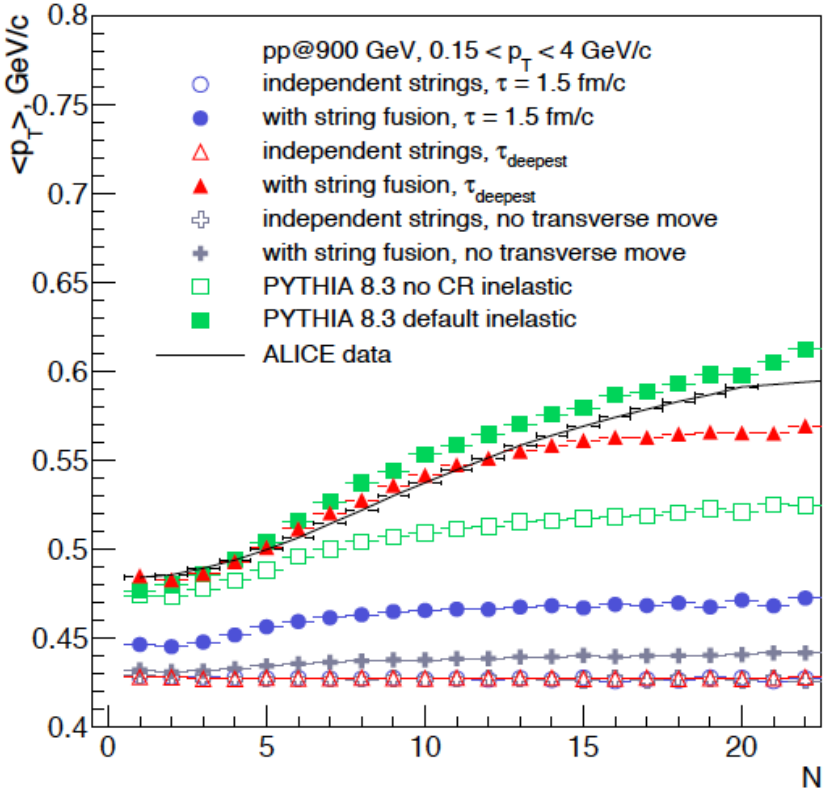

$\langle p_T \rangle$-N_{ch} - корреляции в центральной области быстрот

Рис. 2.8: $\langle p_T \rangle$–N корреляционная функция, вычисленная в аксептансе $|\eta| < 0.8$, $0.15 < p_T < 4$ ГэВ для неупругих $p + p$ взаимодействий при $\sqrt{s} = 900$ ГэВ. Результаты модели для струнной системы, эволюционирующей до τ_{deepest}, представленные полными красными треугольниками, настроены в соответствии с данными ALICE [129] (черная линия: точки данных соединены, чтобы улучшить восприятие). Подробности см. в тексте.

Модель взаимодействующих струн, конечных по быстроте, учитывающая поперечную и продольную динамику (кандидатская Дарьи Прохоровой)

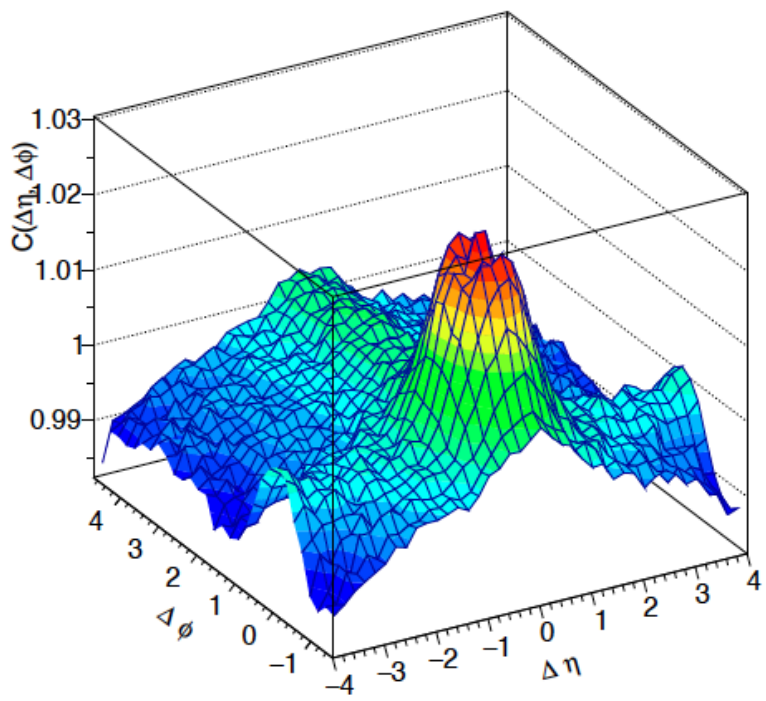

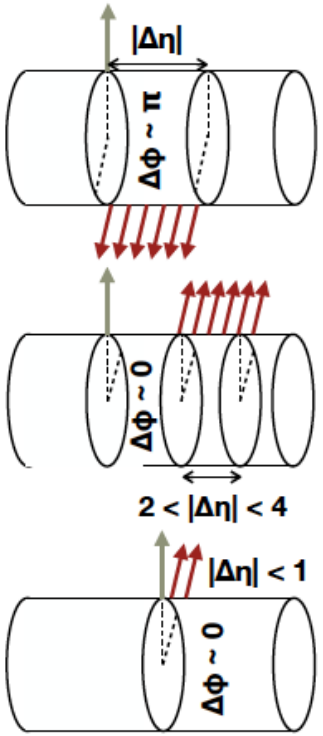

Рис. 3.7: Слева: Модельный результат для двухчастичной корреляционной функции $C(\Delta\eta, \Delta\phi)$, рассчитанной для частиц с $|\eta| < 2.5$ и $0.3 < p_T < 3.0$ ГэВ и представленной для класса событий $0-10\%$ на основе множественности заряженных частиц $N_{\rm ch}^{\rm sel}$ с $|\eta| < 2.5$ и $p_T > 0.6$ ГэВ для неупругих $p+p$ взаимодействий при $\sqrt{s} = 13$ ТэВ. **Справа:** схематическое объяснение наблюдаемых $\Delta\eta - \Delta\phi$ корреляций.

ыстрот

Multiplicity dependence of the average transverse momentum in pp, p–Pb,and Pb–Pb collisions at the LHC☆

ALICE Collaboration

Physics Letters B, Volume 727, Issues 4–5, 18 December 2013, Pages 371-380

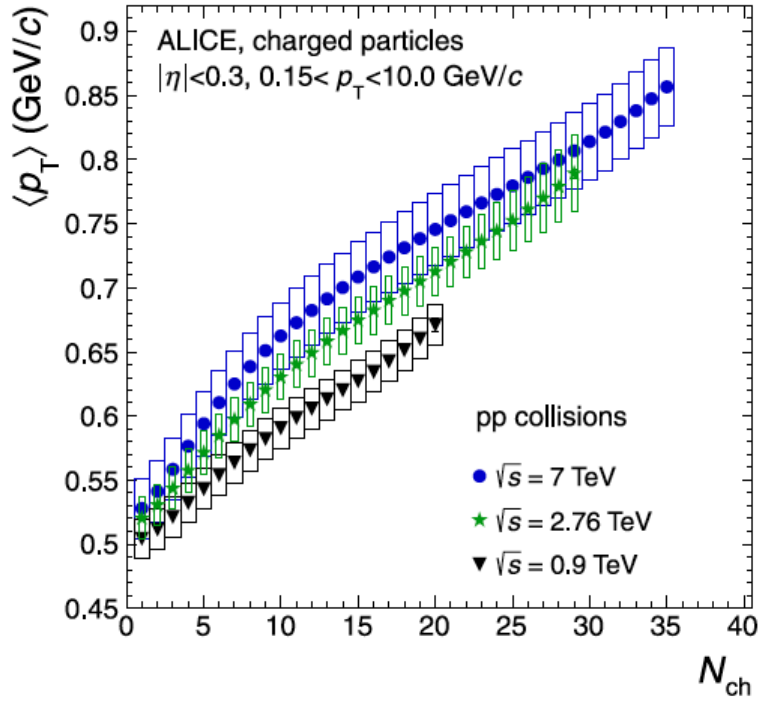

Fig. 1. Average transverse momentum $\langle p_T \rangle$ in the range $0.15 < p_T < 10.0$ GeV/c as a function of charged-particle multiplicity N_{ch} in pp collisions at $\sqrt{s} = 0.9, 2.76$, and 7 TeV, for $|\eta| < 0.3$. The boxes represent the systematic uncertainties on $\langle p_T \rangle$. The statistical errors are negligible.

- $\langle p_T \rangle$-N_{ch} - корреляции в центральной области быстрот
--- а дальние корреляции?

PYTHIA

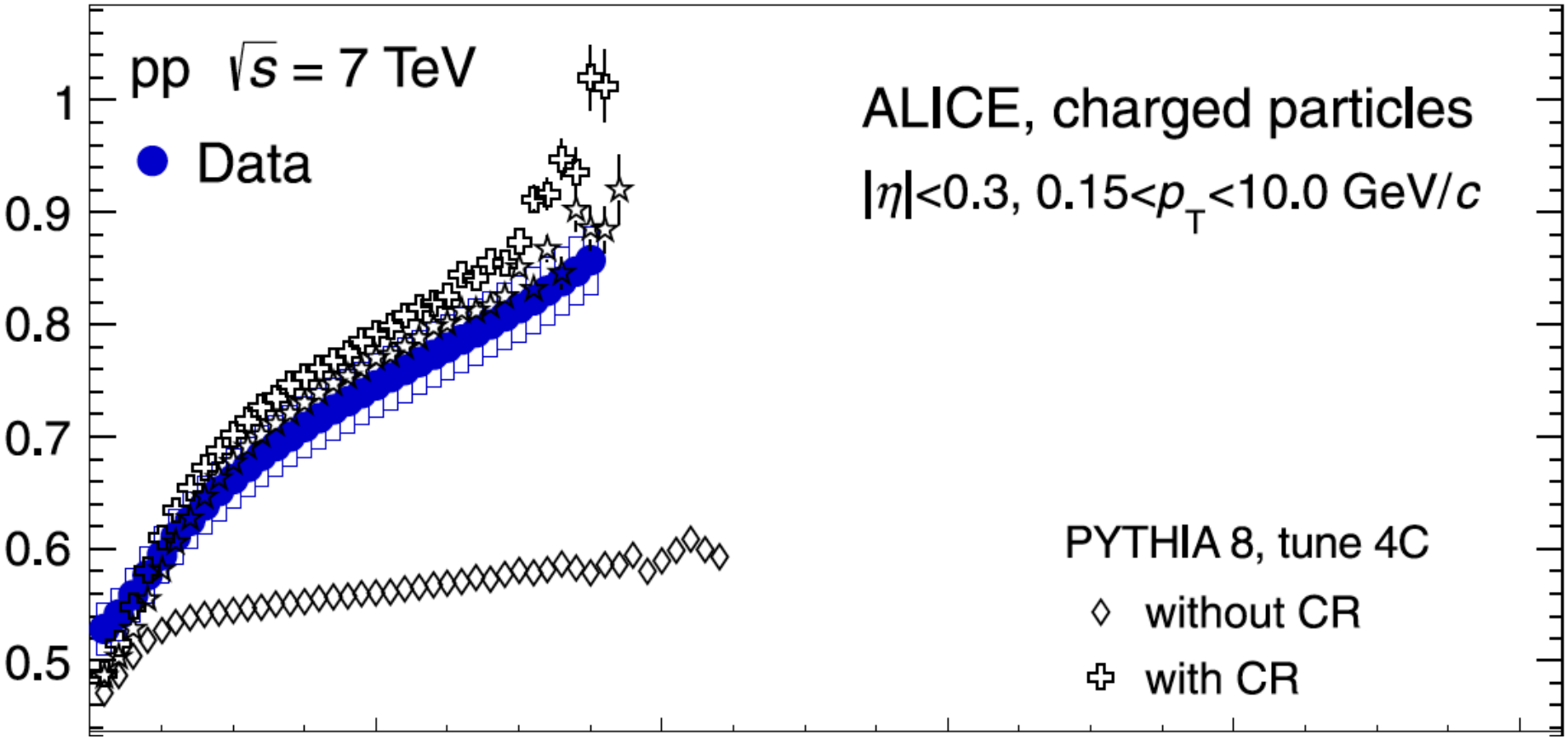
pp $\sqrt{s}$ = 7 TeV
Data
ALICE, charged particles
$|\eta|$<0.3, 0.15<p_T<10.0 GeV/c
PYTHIA 8, tune 4C
without CR
with CR
1
0.9
0.8
0.7
0.6
0.5

Mean p_T in pp, p-Pb and Pb-Pb

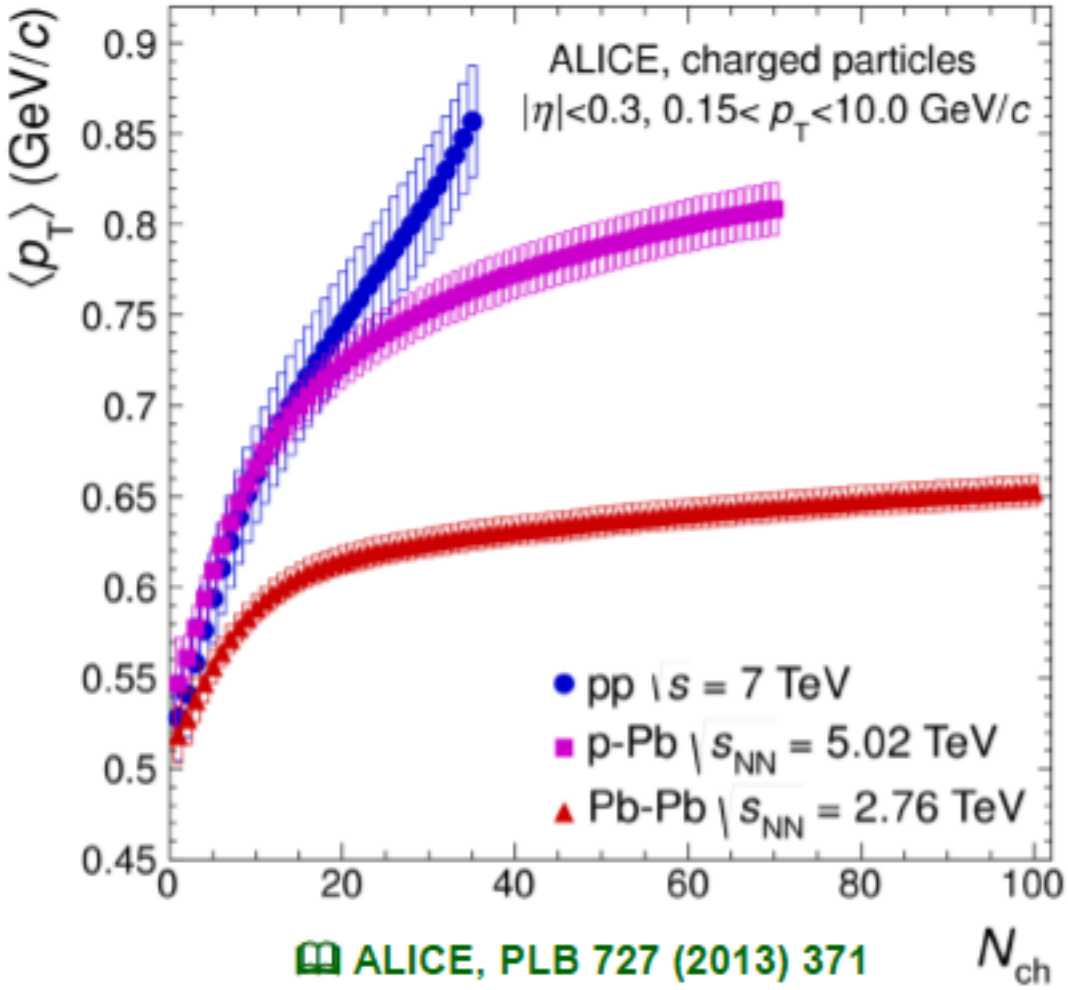

ALICE, PLB 727 (2013) 371

ALI-PUB-55941

- Three different √s for pp, p-Pb and Pb-Pb
  - ⇨ but √s dependence expected to be weak
- Much stronger increase of $\langle p_T \rangle$ in p-Pb than in Pb-Pb
- p-Pb follows pp up to N_{ch}~14-15
- N_{ch}>14 corresponds to
  - ⇨ ~10% of pp x-section:
    - ✓ ***pp already highly biased***
  - ⇨ 50% of p-Pb x-section
    - ✓ ***only centrality bias***

ЕРОХИН Андрей Александрович

Выпускная квалификационная работа
Исследование энергетической зависимости дальних корреляций множественности заряженных частиц в протон-протонных столкновениях в эксперименте ALICE на LHC
Уровень образования: аспирантура

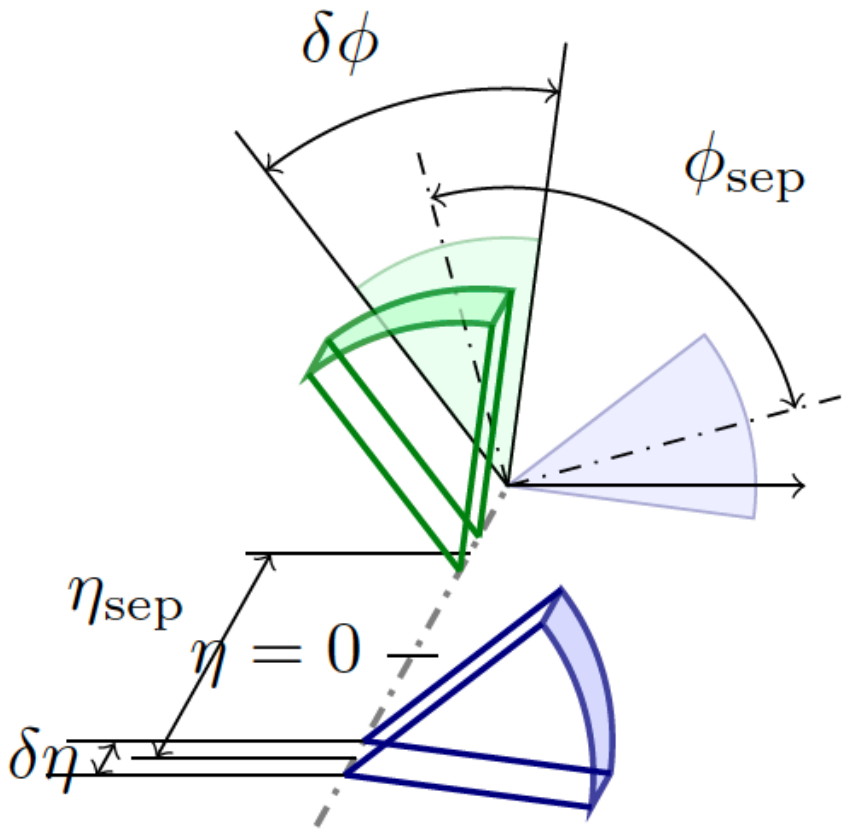

Рис. 6: Схематическое изображение окон, в которых производились измерения корреляций множественности заряженных частиц.

$\sqrt{s_{\text{СМ}}}$, ГэВ	Период pass/AOD	Число отобранных событий
900	LHC10c pass4/AOD221	4 563 735
2760	LHC13g pass1/AOD155	11 349 195
5020	LHC15n pass4/AOD208	99 612 843
7000	LHC10b pass4/AOD221	15 642 255
7000	LHC10d pass4/AOD221	65 100 283
13000	LHC17k pass1/AOD234	85 846 276

Таблица 3: Наборы данных, использованные в анализе

Σ

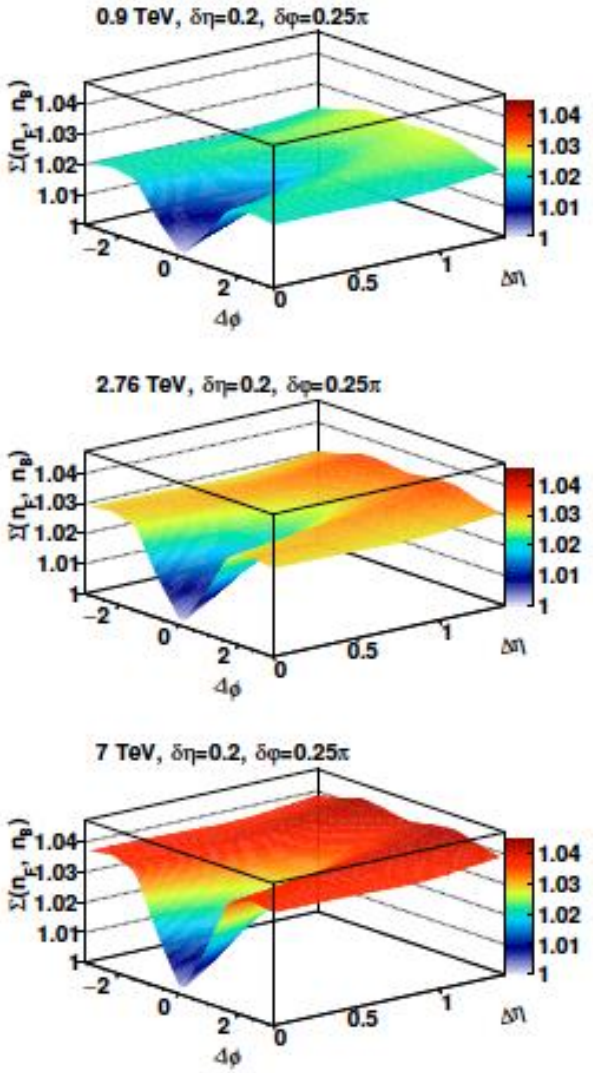

Рис. 2: Сильно интенсивная наблюдаемая $\Sigma(n_F, n_B)$ между множественностями в двух окнах шириной $\delta\eta = 0.2$ и $\delta\varphi = \pi/4$ как функция расстояния между центрами окон $\Delta\eta$ по быстроте и $\Delta\varphi$ по азимуту, рассчитанный в модели с независимыми идентичными строками в статье[31] с использованием двухчастичная корреляционная функция струны $\Lambda(\Delta\eta, \Delta\varphi)$ (6) получено путем фитирования [29] экспериментальных данных pp ALICE [8] по FB корреляциям между множественностями при трех начальных энергиях: 0,9, 2,76 и 7 ТэВ в аксептансе псевдобыстрот ALICE TPC. (Рисунок из статьи [31].)

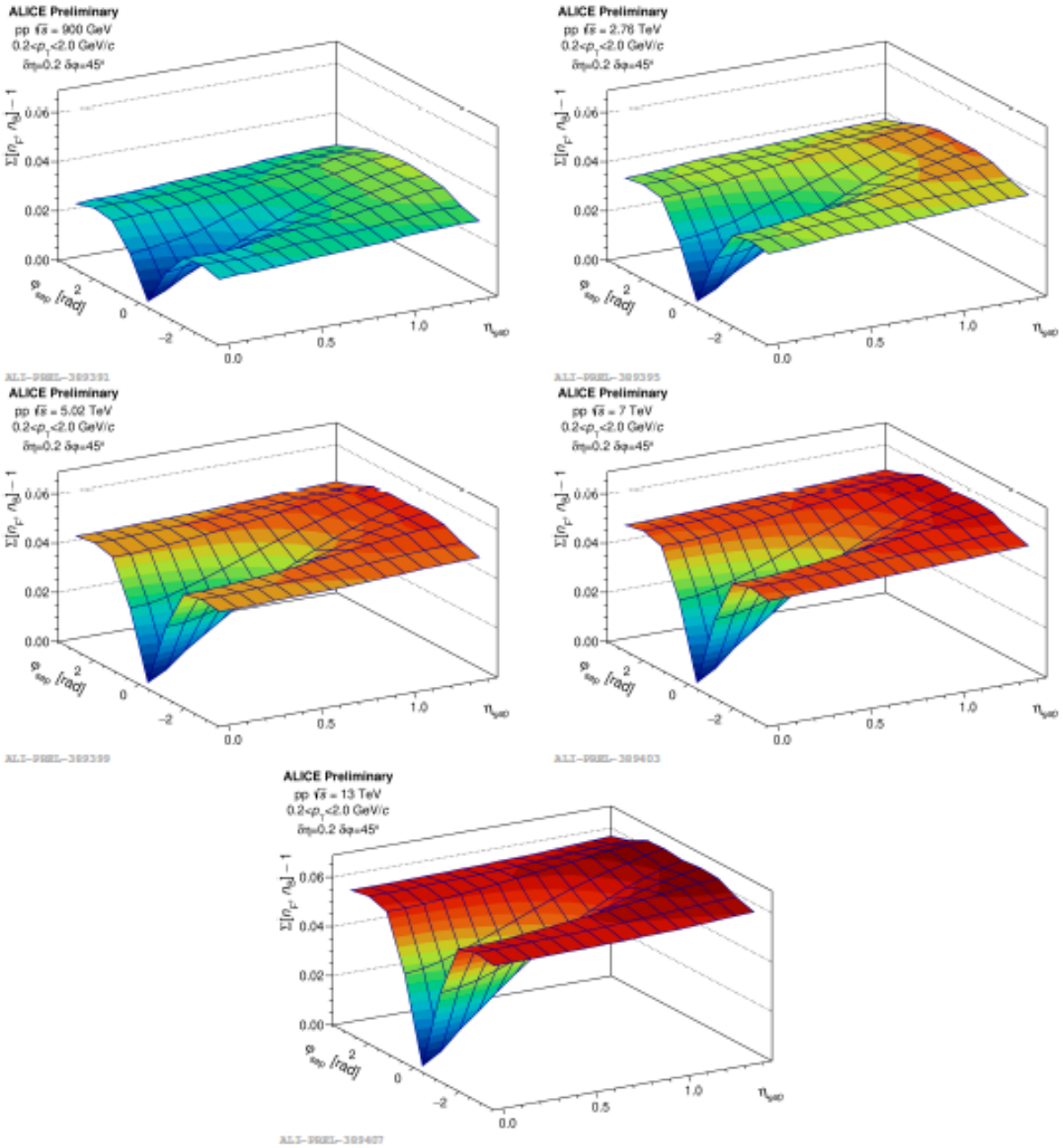

Рис. 9: $\Sigma\left[n_{\mathrm{F}}, n_{\mathrm{B}}\right]-1$ **в зависимости расстояния между центрами двух окон размера** $\delta\eta = 0.2$ $\delta\varphi = 45°$ **для 5 энергий pp столкновений1.**

Поиск нелинейных эффектов в адронных столкновениях на БАК

Магистерская диссертация студента
_____ **Ерохина Андрея Александровича**
Научный руководитель:
_____ к. ф.-м. н., доц. **Г. А. Феофилов**
Рецензент:
_____ к. ф.-м. н., снс. **Е. Л. Крышень**

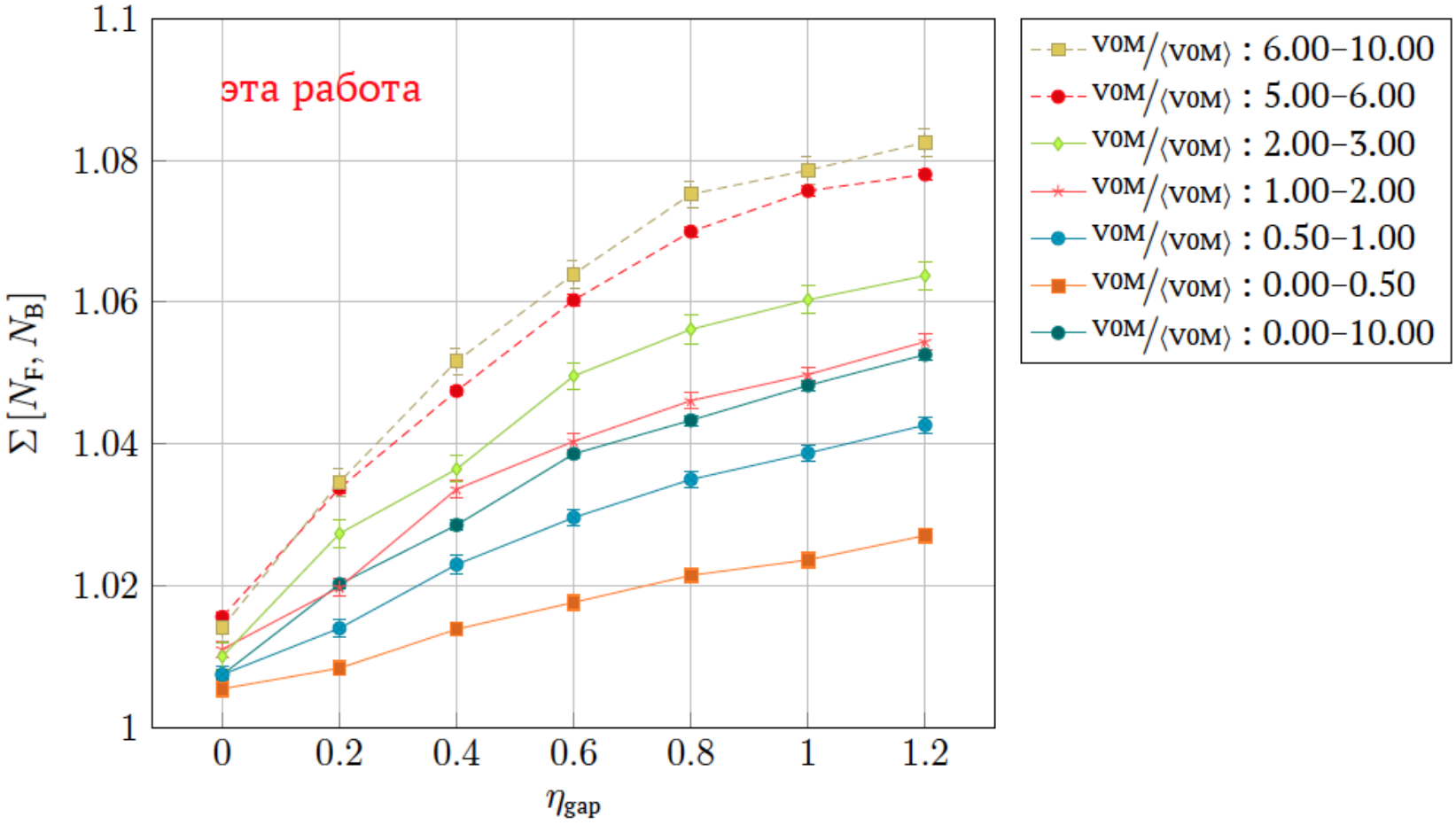

Рисунок 11 – Сечение двумерного графика $\Sigma\,[N_F, N_B]$ в $\varphi_{sep} = 0$ для разных классов по множественности. $0.2\,\text{ГэВ} < p_T < 2.0\,\text{ГэВ}$

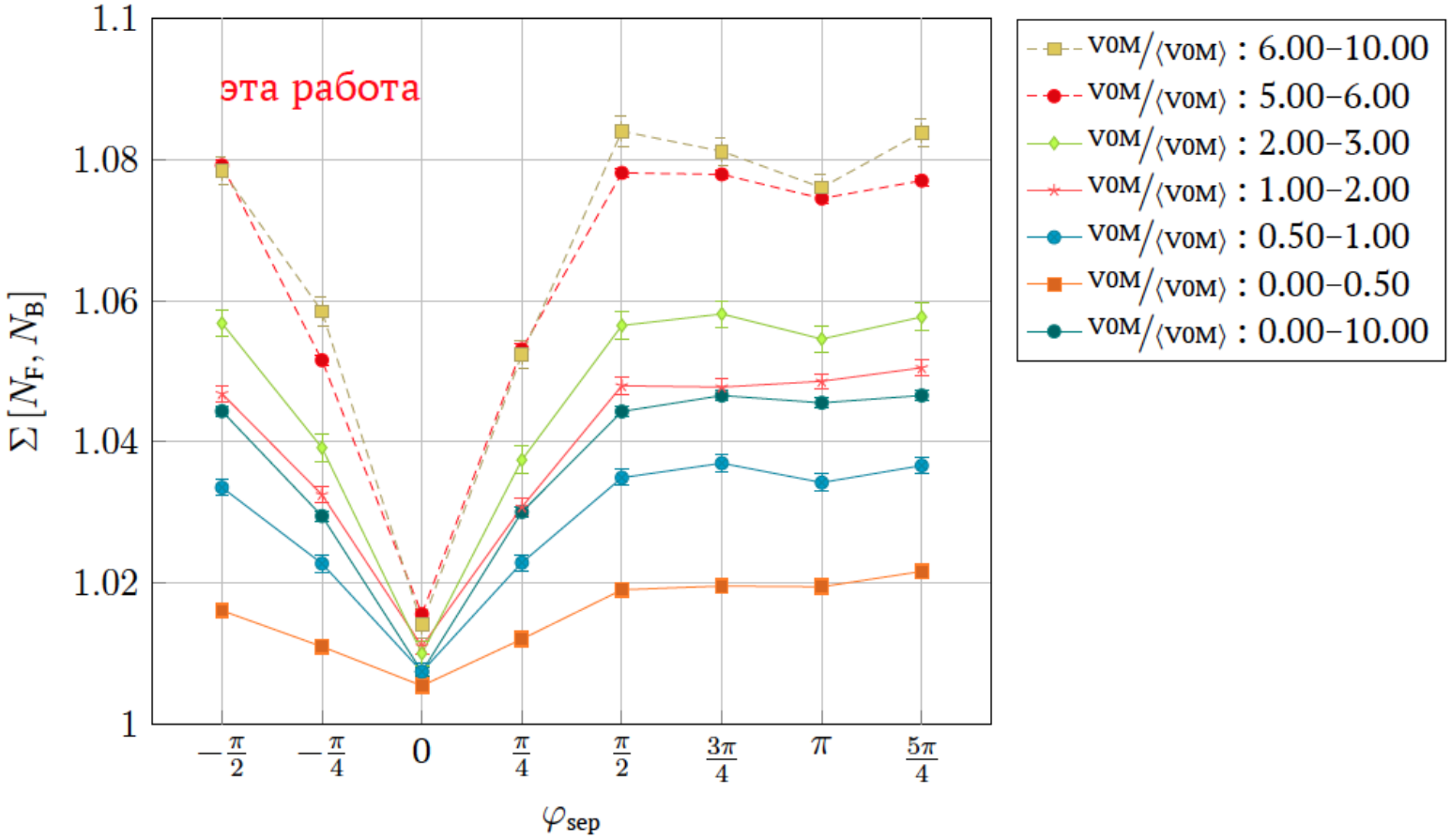

Рисунок 13 – Сечение двумерного графика $\Sigma\,[N_{\mathrm{F}}, N_{\mathrm{B}}]$ в $\eta_{\mathrm{gap}} = 0$ для разных классов по множественности. $0.2\,\text{ГэВ} < p_{\mathrm{T}} < 2.0\,\text{ГэВ}$

Обнаружен нелинейный плато величины $\Sigma\,[N_{\mathrm{F}}, N_{\mathrm{B}}]$ в зависимости от энергии и рост плато для событий с большой множественностью. Для событий с большой множественностью ($5 < {}^{v}/_{\langle v\rangle 0M} < 6$) обнаружена особенность топологии — протяжённый вдоль η_{gap} провал для $\varphi_{\mathrm{sep}} = 0$, который соответствует ближнему риджу в двухчастичных корреляционных функциях.